

Tristetraprolin-driven regulatory circuit controls quality and timing of mRNA decay in inflammation

Franz Kratochvill¹, Christian Machacek¹, Claus Vogl², Florian Ebner¹, Vitaly Sedlyarov¹, Andreas R Gruber³, Harald Hartweger¹, Raimund Vielnascher², Marina Karaghiosoff², Thomas Rüllicke⁴, Mathias Müller^{2,4}, Ivo Hofacker³, Roland Lang⁵ and Pavel Kovarik^{1,*}

¹ Max F. Perutz Laboratories, Center for Molecular Biology, University of Vienna, Vienna, Austria, ² Institute of Animal Breeding and Genetics, University of Veterinary Medicine Vienna, Vienna, Austria, ³ Department of Theoretical Chemistry, University of Vienna, Vienna, Austria, ⁴ Institute of Laboratory Animal Science and Biomodels Austria, University of Veterinary Medicine Vienna, Vienna, Austria and ⁵ Institute of Clinical Microbiology, Immunology and Hygiene, University Hospital Erlangen, Erlangen, Germany

* Corresponding author. Max F. Perutz Laboratories, Center for Molecular Biology, University of Vienna, Vienna 1030, Austria. Tel.: +43 14 277 54608; Fax: +43 14 277 9546; E-mail: pavel.kovarik@univie.ac.at

Received 31.5.11; accepted 7.11.11

For a successful yet controlled immune response, cells need to specifically destabilize inflammatory mRNAs but prevent premature removal of those still used. The regulatory circuits controlling quality and timing in the global inflammatory mRNA decay are not understood. Here, we show that the mRNA-destabilizing function of the AU-rich element-binding protein tristetraprolin (TTP) is inversely regulated by the p38 MAPK activity profile such that after inflammatory stimulus the TTP-dependent decay is initially limited to few mRNAs. With time, the TTP-dependent decay gradually spreads resulting in cumulative elimination of one third of inflammation-induced unstable mRNAs in macrophages *in vitro*. We confirmed this sequential decay model *in vivo* since LPS-treated mice with myeloid TTP ablation exhibited similar cytokine dysregulation profile as macrophages. The mice were hypersensitive to LPS but otherwise healthy with no signs of hyperinflammation seen in conventional TTP knockout mice demonstrating the requirement for myeloid TTP in re-installment but not maintenance of immune homeostasis. These findings reveal a TTP- and p38 MAPK-dominated regulatory mechanism that is vital for balancing acute inflammation by a temporally and qualitatively controlled mRNA decay.

Molecular Systems Biology 7: 560; published online 20 December 2011; doi:10.1038/msb.2011.93

Subject Categories: functional genomics; immunology

Keywords: immune homeostasis; inflammation; mRNA stability; p38 MAPK; tristetraprolin

Introduction

Inflammation-elicited gene expression changes are controlled by mechanisms that allow sufficiently strong responses but restrain the amplitude and interval of altered gene expression to avoid tissue damage and pathological inflammation. Cells achieve this control by employing a number of cell-autonomous positive and negative feedback mechanisms. At the level of gene transcription, this dynamic control was shown to result from regulatory circuits such as those of the transcription factors NF- κ B, C/EBP δ and ATF3 that act as activator, amplifier and attenuator, respectively (Litvak *et al.*, 2009). Another important broad range control of inflammatory gene expression targets mRNA stability (Raghavan and Bohjanen, 2004; Cheadle *et al.*, 2005; Anderson 2010). The rate of mRNA decay was shown to be particularly important for the expression of cytokine and chemokine genes that exhibit the most dynamic expression pattern (Hao and Baltimore, 2009). mRNAs of these genes are enriched in AU-rich elements (AREs) in their 3' untranslated regions (UTRs) confirming the prominent role of AREs in mRNA stability (Barreau *et al.*, 2005). The regulatory circuits coordinating global ARE-mediated decay are not well understood. The stability of ARE-containing

mRNAs is regulated by the recruitment of stabilizing or destabilizing ARE-binding proteins that facilitate or prevent contact with RNA-degrading complexes (Barreau *et al.*, 2005; Stoecklin and Anderson, 2007). The complexity and dynamics of ARE-mediated mRNA stability is increased by combinatorial effects of ARE-binding proteins (Mukherjee *et al.*, 2009). Coupling between translation and mRNA degradation as well as cooperation of RNA-binding proteins with microRNAs contribute to the global mRNA stability control (Chekulaeva and Filipowicz, 2009; Dahan *et al.*, 2011). TTP, which is encoded by the *Zfp36* gene, is one of the best-characterized ARE-binding proteins. After binding to AREs, TTP initiates the assembly of the mRNA degradation machinery thereby causing elimination of the bound mRNAs (Carballo *et al.*, 1998; Blackshear, 2002; Sandler and Stoecklin, 2008). TTP was initially characterized as a key inflammation-induced *Tnf* mRNA-destabilizing factor whose deficiency resulted in multiple chronic inflammatory syndromes including arthritis, cachexia and dermatitis in mice (Taylor *et al.*, 1996). Notably, TTP deficiency does not lead to any developmental defects, which contrasts the essential function of the TTP-related genes *Zfp36l1* and *Zfp36l2* in animal development and in the control of cell proliferation (Hodson *et al.*, 2010). The phenotype of the

TTP-deficient mice remains incompletely understood particularly with respect to the growing number of TTP targets. The function of TTP during inflammatory responses *in vivo* has not been explored.

In this study, we employed a global mRNA stability assay to demonstrate TTP as non-redundant component of a negative feedback mechanism that sequentially targets one third of intrinsically unstable inflammation-induced mRNAs for timely degradation in macrophages. This regulatory circuit is controlled by the dual function of p38 MAPK in the regulation of TTP activity. p38 MAPK is known to be needed for TTP expression but in parallel it restrains the mRNA-destabilizing activity of TTP (Sandler and Stoecklin, 2008). We show that the p38 MAPK activity profile during inflammatory response qualitatively and temporally controls TTP-driven ARE-dominated mRNA decay such that a premature degradation of inflammatory mRNAs is prevented until the onset of the resolution phase of the inflammatory response. We show the ability of this TTP- and p38 MAPK-dominated regulatory system to determine which mRNAs are degraded at a certain time in macrophages. To demonstrate the function of this regulatory system *in vivo*, we generated mice deficient in myeloid TTP. In response to LPS, these mice displayed temporal dysregulation of cytokine production resembling defects seen in TTP-deficient macrophages. The mice were hypersensitive to LPS-induced endotoxin shock. However, under normal conditions the animals were healthy and fertile, indicating that myeloid TTP has an essential role in the negative feedback upon inflammatory stimulus rather than in the originally proposed maintenance of immune homeostasis under steady-state conditions.

Results

Genome-wide analysis of mRNA stability in LPS-stimulated WT and TTP^{-/-} macrophages

Because of their functions as sensors and effectors of inflammation, macrophages are often used to study inflammatory gene expression patterns (Hume *et al*, 2007). Macrophages stimulated with Toll-like receptor (TLR) ligands exhibit highly dynamic gene expression profiles in terms of both the magnitude and timing. To address the timely removal of inflammation-induced mRNAs in these cells, we examined the global effect of TTP on mRNA decay rates by microarray-based measurement of remnant mRNA after transcriptional blockade with actinomycin D (act D) in LPS-treated bone marrow-derived macrophages (BMDMs) from WT and conventional knockout (TTP^{-/-}) mice (Taylor *et al*, 1996). Previous screens were not successful in the identification of one or more of the few already known TTP targets such as *Tnf*, the best-characterized TTP target (Lai *et al*, 2006; Emmons *et al*, 2008; Stoecklin *et al*, 2008). To increase the sensitivity of the mRNA decay profiling, we pharmacologically inhibited the LPS-activated p38 MAPK (using the specific p38 MAPK inhibitor SB203580) at the time of transcriptional blockade by act D. Although p38 MAPK is required for TTP expression and TTP protein stability, at the same time it inhibits the mRNA-destabilizing activity of TTP (Sandler and Stoecklin, 2008). The pharmacological inhibition of p38 MAPK mimics

an intrinsic inhibitory pathway that is driven by IL-10 and the IL-10-induced phosphatase *Dusp1* that gradually inactivates p38 MAPK (Hammer *et al*, 2005). BMDMs from WT and TTP^{-/-} animals were stimulated for 3 h with LPS followed by simultaneous treatment with act D and SB203580. The remnant mRNA levels were measured at 45 and 90 min thereafter. The 3-h treatment with LPS was sufficient to induce high levels of TTP protein that remained detectable even 90 min after the transcriptional block, and despite degradation caused by the inhibition of p38 MAPK (Supplementary Figure 1). After normalization, filtering and statistical analysis of the microarray data, the probe set IDs of the remaining genes (9847 from total 28 853 present on the chip) were classified according to two criteria: (1) mRNA decay significantly ($P < 0.05$) increased above the overall average of the data set in WT cells and (2) significantly ($P < 0.05$) slower decay in TTP^{-/-} compared with WT cells. Approximate half-lives of the mRNAs are also shown (Table I; Supplementary Table 1). The half-lives were calculated individually for each gene using the signal differences between 0 and 90 min of act D treatment. The 45-min act D time point was not considered for half-life calculations since the difference in means was low compared with the variation at this time point. The single criterion for classification of an mRNA as unstable or TTP destabilized was the P -value, which also incorporated inversely the gene-specific standard error, instead of the half-life, which did not (Materials and methods). Among the 9847 genes, 1090 (10%) were found to be significantly unstable (Supplementary Table 1), with the 25 most significantly unstable genes listed in Table IA. Of the 1090 unstable mRNAs, 309 transcripts (28%) displayed significantly increased stability in TTP^{-/-} cells (Supplementary Table 1). Most of the so far known TTP targets were present in this group (Table IB; Supplementary Table 1) while those not found in our screen are known to be expressed in other cell types than in BMDMs, i.e., in T cells (*Il2*, *Ifng*), B cells (*E47*) or mast cells (*Il3*) (Carballo *et al*, 2000; Stoecklin *et al*, 2003, 2008; Tchen *et al*, 2004; Ogilvie *et al*, 2005, 2009; Chen *et al*, 2006; Lai *et al*, 2006; Frasca *et al*, 2007; Datta *et al*, 2008; Horner *et al*, 2009; Tudor *et al*, 2009; Zhao *et al*, 2011). Several of the known TTP targets did not rank among the top 25 unstable mRNAs though they all displayed TTP-dependent decays with P -values < 0.05 in our analysis (Table I). Within the 25 most unstable mRNAs only three were not destabilized in a TTP-dependent manner (Table IA) emphasizing the fundamental role of TTP particularly in the removal of the short-lived messages. Increased mRNA stability in TTP^{-/-} BMDMs can be also caused by an indirect involvement of TTP, e.g., by an mRNA-stabilizing protein that may be more abundant in TTP^{-/-} cells. To test the direct involvement of TTP, we selected the mRNAs of *Il1a* and *Cxcl2* (GenBank IDs: NM_010554 and NM_009140, respectively) for a comprehensive analysis. The P -values for TTP-mediated decays and the half-lives of these mRNAs ranged from being strong (*Cxcl2*) to modest (*Il1a*) dependent on TTP (Table IB). Verification of the microarray data by quantitative RT-PCR (qRT-PCR) under same experimental conditions (i.e., in the presence of p38 MAPK inhibitor) confirmed that *Il1a* and *Cxcl2* were degraded in a TTP-dependent manner (Figure IA). Analysis of the 3' UTRs of the two mRNAs using AREsite (Gruber *et al*, 2011) revealed that they contained several

Table 1 Decay of most significantly unstable mRNAs is TTP dependent

(A) Top 25 transcripts displaying most significant instability values.

Nr.	mRNA accession nr.	Gene name	P-value for decay in WT	P-value for TTP-dependent decay	Half-life in WT (min)	Half-life in TTP ^{-/-} (min)
1	NM_013693	<i>Tnf</i>	0.000	0.000	21	208
2	NM_009404	<i>Tnfsf9</i>	0.000	0.000	29	65
3	NM_010104	<i>Edn1</i>	0.000	0.001	31	54
4	NM_152804	<i>Plk2</i>	0.000	0.003	25	43
5	NM_011756	<i>Zfp36</i>	0.000	0.000	24	60
6	NM_008176	<i>Cxcl1</i>	0.000	0.000	31	567
7	NM_007707	<i>Socs3</i>	0.000	0.007	24	38
8	NM_009397	<i>Tnfaip3</i>	0.000	0.041	28	39
9	NM_010907	<i>Nfkb1a</i>	0.000	0.005	26	45
10	NM_008348	<i>Il10ra</i>	0.000	0.000	40	130
11	NM_007746	<i>Map3k8</i>	0.000	0.009	36	58
12	NM_175666	<i>Hist2h2bb</i>	0.000	0.000	42	89
13	NM_053109	<i>Clec2d</i>	0.000	0.061	33	44
14	NM_009140	<i>Cxcl2</i>	0.000	0.000	47	Stable
15	NM_017373	<i>Nfil3</i>	0.000	0.001	38	75
16	NM_020034	<i>Hist1h1b</i>	0.000	0.194	37	48
17	NM_008416	<i>Junb</i>	0.000	0.004	36	66
18	NM_030609	<i>Hist1h1a</i>	0.000	0.043	47	65
19	BC011440	<i>LOC665622</i>	0.000	0.037	45	68
20	NM_007679	<i>Cebpd</i>	0.000	0.096	44	60
21	NM_019873	<i>Fkbp1</i>	0.000	0.008	48	81
22	NM_018820	<i>Sertad1</i>	0.000	0.005	41	83
23	NM_178199	<i>Hist1h2bl</i>	0.000	0.025	44	70
24	NM_010500	<i>Ier5</i>	0.000	0.003	40	86
25	NM_178201	<i>Hist1h2bn</i>	0.000	0.037	46	71

(B) Reported TTP targets and targets characterized in detail in this study

Nr.	mRNA accession nr.	Gene name	P-value for decay in WT	P-value for TTP-dependent decay	Half-life in WT (min)	Half-life in TTP ^{-/-} (min)	Reference
1	NM_013693	<i>Tnf</i>	0.000	0.000	21	208	Taylor et al (1996)
5	NM_011756	<i>Zfp36</i>	0.000	0.000	24	60	Tchen et al (2004)
6	NM_008176	<i>Cxcl1</i>	0.000	0.000	31	567	Datta et al (2008)
14	NM_009140	<i>Cxcl2</i>	0.000	0.000	47	Stable	This study and Jalonen et al (2006)
34	NM_133662	<i>Ier3</i>	0.000	0.008	39	63	Lai et al (2006)
58	NM_009969	<i>Csf2</i>	0.000	0.002	36	82	Carballo et al (2000)
89	NM_010548	<i>Il10</i>	0.000	0.001	28	151	Stoecklin et al (2008)
131	NM_010554	<i>Il1a</i>	0.000	0.004	73	355	This study
164	NM_031168	<i>Il6</i>	0.000	0.005	77	269	Tudor et al (2009); Zhao et al (2011)
216	NM_008361	<i>Il1b</i>	0.000	0.011	102	Stable	Chen et al (2006)

(A) P-values for stability in WT cells and for TTP-dependent decay are shown. Half-lives that were calculated on the basis of mRNA decay within 90 min after transcriptional stop serve for visualization of the P-values. In all, 22 out of 25 unstable mRNAs are degraded in a TTP-dependent decay (highlighted in gray), whereas only three transcripts (*Clec2d*, *Hist1h1b* and *Cebpd*) are destabilized independently of TTP. (B) Data for reported TTP targets and targets characterized in detail in this study (i.e., *Cxcl2* and *Il1a*) are depicted.

AUUUA pentamers representing a minimal ARE, and several UAUUUUAU heptamers, the core TTP binding site (Lai et al, 2006; Supplementary Figure 2A). To test TTP binding to RNA *in vitro*, RNA oligonucleotides comprising the conserved AREs (Supplementary Figure 2B) were examined for their ability to compete with the *Tnf* ARE, a well-characterized TTP-binding sequence (Blackshear et al, 2003), for TTP binding in RNA electrophoretic mobility shift assay (RNA-EMSA) experiments. The conserved AREs of the selected mRNAs were all able to compete with the *Tnf* ARE confirming their binding to TTP (Figure 1B). To prove that TTP conferred instability to the two targets through their 3' UTRs, and to exclude secondary effects of the general transcriptional blockade by act D (e.g., by blocking transcription of genes encoding labile RNases), we fused the 3' UTRs of the chosen mRNAs to a tetracycline-regulated β -globin reporter (Ogilvie et al, 2005). HeLa Tet-Off cells were co-transfected with a TTP expression construct and the 3' UTR reporters. After

shutting off transcription by tetracycline, TTP accelerated the decay of the two targets whereas the stability of the control reporter (3' UTR of *Hprt*) remained unaffected (Figure 1C). All these independent assays confirmed *Cxcl2* and *Il1a* to be TTP targets in BMDMs. Previous reports describing *Il1a* and *Cxcl2* as TTP targets (Jalonen et al, 2006; Tudor et al, 2009) were based only on one type of assay which, if employed individually, may not be sufficient to unambiguously define TTP targets. To further validate the results of our screen, we demonstrated binding of several novel targets (*Ccl2*, *Ccl4*, *Ccl7*, *Cxcl2*, *Ets2*, *Il1a*, *Junb*, *Plaur* and *Tnfsf9*) to TTP by RNA immunoprecipitation (Figure 1D). *Tnf* and *Il6* served as positive and *Hprt* as negative controls. Extracts from LPS-treated WT and, for control, TTP^{-/-} BMDMs were incubated with antibody to TTP or control preimmune serum. The bound RNA was isolated, reverse transcribed and used for RT-PCR to demonstrate binding to TTP. Cumulatively, these data support the concept that our microarray-based mRNA

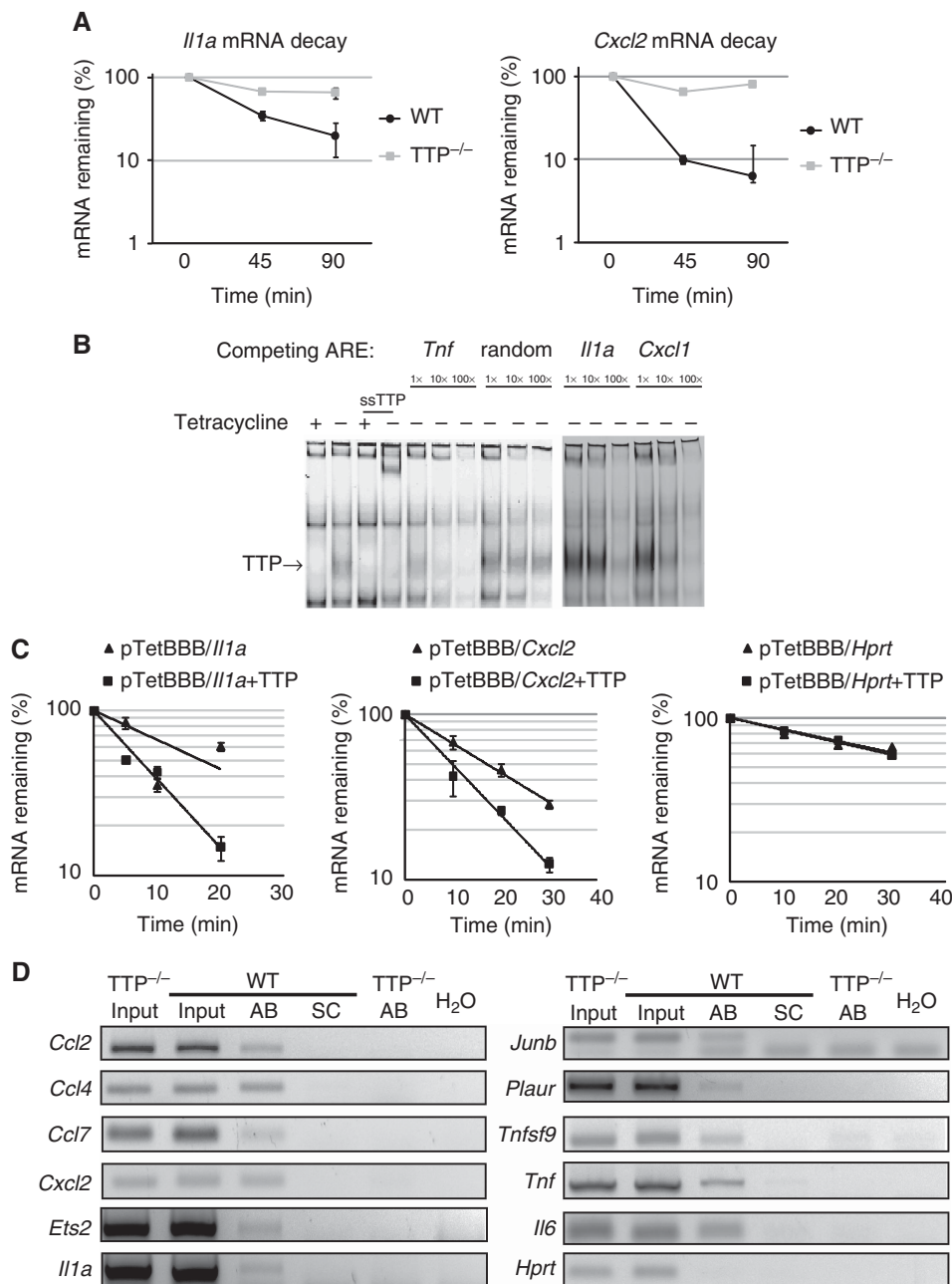


Figure 1 Characterization of *Il1a* and *Cxcl2* mRNAs as TTP targets. **(A)** TTP destabilizes mRNA of *Il1a* and *Cxcl2* in a p38 MAPK-dependent way. WT (TTP^{+/+}) and TTP^{-/-} BMDMs were stimulated for 3 h with LPS followed by transcriptional blockage with act D in the presence of the p38 MAPK inhibitor SB203580 (SB). Decay rates of *Il1a* and *Cxcl2* were monitored by qRT-PCR at the indicated time points. Remnant *Il1a* and *Cxcl2* mRNAs in percent of the amount at the time point of act D treatment is depicted; s.e.m. is shown ($n=3$). **(B)** TTP binds to conserved AREs within the 3' UTR of *Il1a* and *Cxcl2*. HeLa Tet-Off cells were transfected with tetracycline-controlled expression plasmid for Flag-tagged TTP. TTP expression was activated or blocked by cultivating the cells overnight in the absence or presence of tetracycline, respectively. Extracts containing TTP (-tetracycline) or without TTP (+tetracycline) were assayed by RNA-EMSA for binding to Cy5.5-labeled *Tnf* ARE. For competition experiments, 1 ×, 10 × or 100 × excess of unlabeled *Tnf* ARE, a random RNA sequence, *Il1a* ARE or *Cxcl2* ARE was added 20 min after the labeled *Tnf* ARE. The complexes were incubated for additional 20 min and loaded onto the gel. The identity of TTP-containing complexes was confirmed by supershift (ssTTP) using Flag antibody. **(C)** 3' UTRs of *Il1a* and *Cxcl2* confer TTP-dependent instability. HeLa Tet-Off cells were transfected with reporter plasmids containing tetracycline-regulated β -globin fused to 3' UTRs of *Il1a* (pTetBBB/*Il1a*), *Cxcl2* (pTetBBB/*Cxcl2*) and the control *Hprt* (pTetBBB/*Hprt*) together with pCMV-TTP or empty pCMV vector. Twenty-four hours after transfection, tetracycline was added to stop the reporter gene transcription and RNA was isolated at the times indicated. Remnant mRNA is shown in percent of the amount at the time point of transcription stop. Values at each time point represent the mean and s.e.m. of independent experiments ($n=3$). **(D)** TTP interacts with the novel targets *Ccl2*, *Ccl4*, *Ccl7*, *Cxcl2*, *Ets2*, *Il1a*, *Junb*, *Plaur*, *Tnfrsf9*, and the known targets *Tnf* and *Il6* but not with the negative control *Hprt*. WT or TTP^{-/-} BMDMs were treated with LPS for 4 h and the cell lysates were used for RNA immunoprecipitation with TTP antibody (AB) or preimmune serum control (SC). Input control sample was taken before immunoprecipitation. Immunoprecipitated RNA was analyzed by RT-PCR. H₂O control contains no template. Note: *Junb*-specific PCR product is the upper band whereas the lower band represents unused PCR primers that are most strongly visible in the H₂O control. The data are representative of three independent experiments. Source data is available for this figure in the Supplementary Information.

decay analysis identified most of the TTP target mRNAs present in cells after 3 h of LPS treatment (Figure 2A; Supplementary Table 1).

Removal of one third of unstable mRNAs in LPS-induced macrophage transcriptome depends on TTP

To estimate the selective contribution of TTP to the overall decline of inflammatory response after TLR stimulation,

we calculated mRNA stability only for the LPS-induced genes. Expression of these genes was recently shown to be strongly controlled by mRNA stability (Hao and Baltimore, 2009). The transcripts with the most dynamic expression profile, i.e., those showing a rapid and transient induction, were particularly robustly regulated at the level of mRNA stability. To examine the role of TTP in the stability of these early inflammatory mRNAs, we selected LPS-induced genes from our recently published data set of the LPS-induced

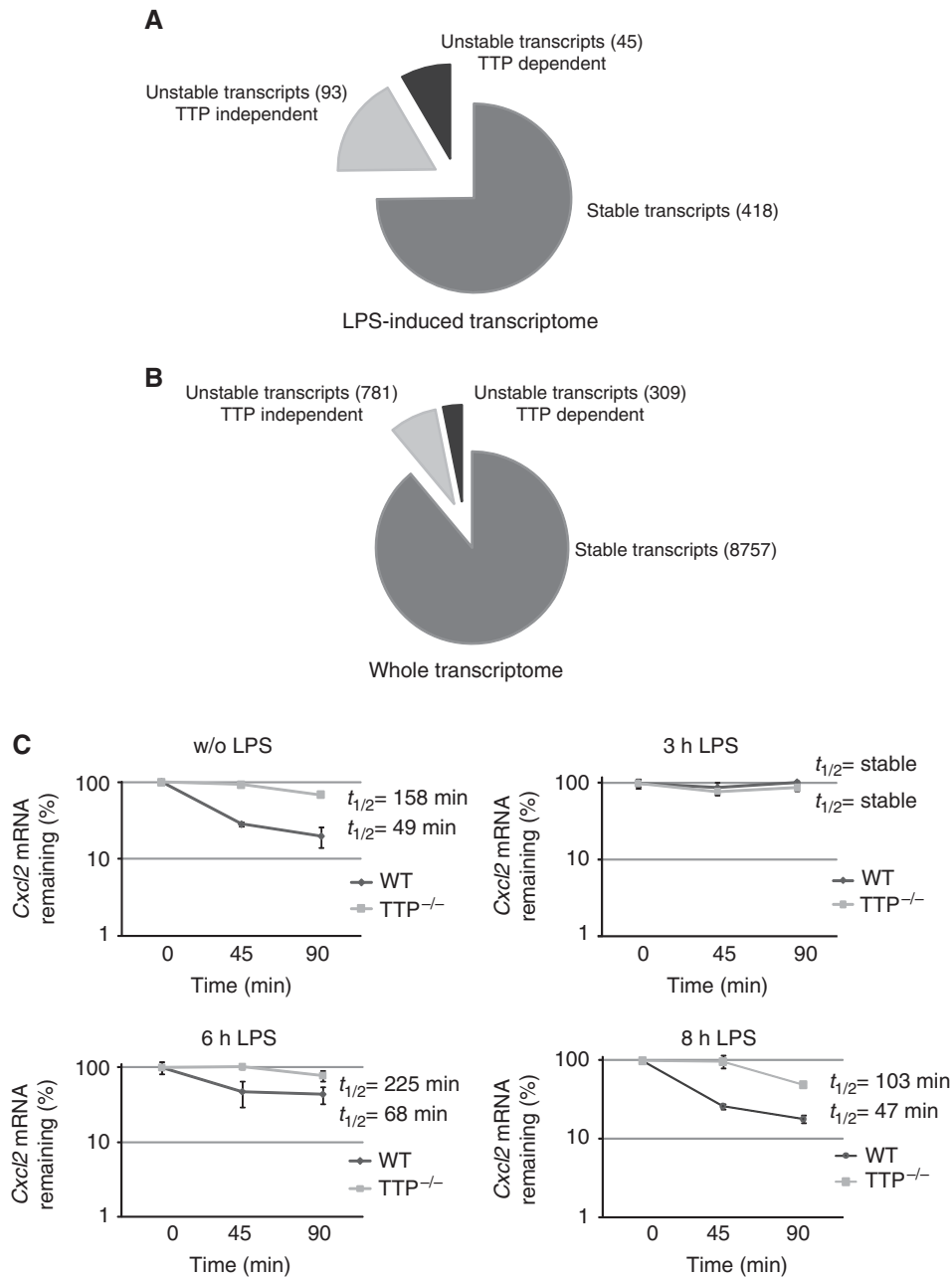


Figure 2 mRNA stability and TTP-dependent mRNA decay in the whole and LPS-induced transcriptome, and Cxcl2 mRNA stability profile during LPS response. **(A)** mRNA stability of LPS-induced transcripts. Unstable mRNAs represent 25% of LPS-induced transcripts (138 out of 546) illustrating that unstable mRNAs are enriched in LPS-induced transcriptome compared with whole transcriptome in **(A)** (25:10%). Out of the 138 unstable mRNAs, 45 (33%) are destabilized by TTP. **(B)** mRNA stability in the whole transcriptome. Within 9847 transcripts, 1090 (10%) are unstable. Out of the 1090 unstable transcripts, 309 (28%) mRNAs display TTP-dependent decay. **(C)** Cxcl2 mRNA becomes destabilized in a TTP-dependent manner after prolonged LPS treatment. WT and TTP^{-/-} BMDMs were left unstimulated or were stimulated for 3, 6 or 8 h with LPS followed by transcriptional blockage with act D. Decay rate of Cxcl2 was monitored by qRT-PCR at the indicated time points. Remnant Cxcl2 mRNA in percent of the amount at the time point of act D treatment is depicted; s.e.m. is shown ($n=3$). Source data is available for this figure in the Supplementary Information.

Table II LPS-induced mRNAs destabilized by TTP

Nr.	mRNA accession nr.	Gene name	<i>P</i> -value for decay in WT	<i>P</i> -value for TTP-dependent decay	Half-life in WT (min)	Half-life in TTP ^{-/-} (min)	Induction by LPS (fold)
1	NM_013693	<i>Tnf</i>	0.000	0.000	21	208	4.52
2	NM_008176	<i>Cxcl1</i>	0.000	0.000	31	567	5.83
3	NM_009140	<i>Cxcl2</i>	0.000	0.000	47	Stable	24.42
4	NM_009404	<i>Tnfsf9</i>	0.000	0.000	29	65	3.55
5	NM_010104	<i>Edn1</i>	0.000	0.001	31	54	3.2
6	NM_017373	<i>Nfil3</i>	0.000	0.001	38	75	15.1
7	NM_008416	<i>Junb</i>	0.000	0.004	36	66	3.23
8	NM_010907	<i>Nfkbia</i>	0.000	0.005	26	45	3.65
9	NM_007707	<i>Socs3</i>	0.000	0.007	24	38	5.37
10	NM_007746	<i>Map3k8</i>	0.000	0.009	36	58	7.31
11	NM_009397	<i>Tnfaip3</i>	0.000	0.041	28	39	9.8
12	NM_009895	<i>Cish</i>	0.000	0.000	34	129	100.62
13	NM_008654	<i>Myd116</i>	0.000	0.001	48	117	3.67
14	NM_133662	<i>Ier3</i>	0.000	0.008	39	63	3.51
15	NM_009969	<i>Csf2</i>	0.000	0.002	36	82	3.86
16	NM_172911	<i>D8Erd82e</i>	0.000	0.014	57	87	7.02
17	NM_153287	<i>Axud1</i>	0.000	0.017	38	78	4.81
18	NM_008842	<i>Pim1</i>	0.000	0.000	73	381	8.73
19	NM_010548	<i>Il10</i>	0.000	0.001	28	151	3.41
20	NM_153159	<i>Zc3h12a</i>	0.000	0.017	62	108	3.13
21	NM_175045	<i>Bcor</i>	0.000	0.005	82	224	4.83
22	NM_010554	<i>Il1a</i>	0.000	0.004	73	355	49.23
24	NM_015790	<i>Icosl</i>	0.000	0.014	92	411	8.51
23	NM_031168	<i>Il6</i>	0.000	0.005	77	269	5.83
25	NM_011333	<i>Ccl2</i>	0.000	0.005	85	409	3.81
26	NM_010755	<i>Maff</i>	0.000	0.001	95	Stable	94.21
27	NM_013652	<i>Ccl4</i>	0.000	0.005	106	Stable	4.54
28	NM_033601	<i>Bcl3</i>	0.000	0.013	106	422	4.16
29	NM_031252	<i>Il23a</i>	0.000	0.003	109	Stable	4.92
30	NM_008361	<i>Il1b</i>	0.000	0.011	102	Stable	5.54
31	NM_013822	<i>Jag1</i>	0.000	0.006	114	Stable	8.78
32	NM_001081298	<i>Lphn2</i>	0.000	0.000	81	Stable	3.01
33	NM_011113	<i>Plaur</i>	0.001	0.008	136	Stable	167.55
34	NM_153537	<i>Phldb1</i>	0.001	0.030	127	415	52.95
35	NM_008057	<i>Fzd7</i>	0.001	0.017	117	Stable	3.92
36	NM_013654	<i>Ccl7</i>	0.001	0.031	117	454	8.85
37	NM_011337	<i>Ccl3</i>	0.001	0.011	184	Stable	14.94
38	NM_198600	<i>Pols</i>	0.001	0.008	106	Stable	4.12
39	NM_011809	<i>Ets2</i>	0.002	0.023	147	Stable	3.04
40	NM_011198	<i>Ptgs2</i>	0.004	0.038	139	Stable	4.15
41	NM_010731	<i>Zbtb7a</i>	0.006	0.045	150	Stable	10.13
42	NM_019835	<i>B4galt5</i>	0.008	0.042	196	Stable	8.21
43	NM_172572	<i>Rhbdp2</i>	0.010	0.027	189	Stable	25.03
44	NM_010493	<i>Icam1</i>	0.014	0.014	247	Stable	4.55
45	NM_178644	<i>Oaf</i>	0.025	0.011	222	Stable	8.4

In all, 45 out of 138 unstable LPS-induced transcripts are destabilized in TTP-dependent manner. TTP-dependent decay was defined by *P*-values <0.05 for decay differences between WT and TTP^{-/-} cells. The transcripts are ordered according to their *P*-values for decay in WT cells. Calculated half-lives support the visualization of the *P*-values.

transcriptome (Mages *et al*, 2007) and compared their mRNA stability using the mRNA decay data set. Transcripts induced at least three-fold after stimulation with LPS for 3 h were considered as LPS induced. Out of 546 LPS-induced transcripts, 138 transcripts (25%) were classified as significantly unstable (Figure 2A). Thus, unstable transcripts were enriched in the LPS-induced transcriptome compared with the whole transcriptome (25 versus 10%) (Figure 2B). Transcripts displaying TTP-dependent decay represented 33% of the unstable LPS-induced mRNAs revealing a key role of TTP in the removal of inflammatory mRNAs (Figure 2A; Table II; Supplementary Table 2). Apart from the known TTP targets (e.g., *Tnf*, *Il10*, *Cxcl1*, *Il1b*, and *Il6*) and those described in more detail in this study (*Il1a* and *Cxcl2*), several other important mediators of inflammation were found among the LPS-

induced TTP-destabilized transcripts. These include *Ccl2*, *Ccl3*, *Ccl4* and *Il23* (Table II). While these transcripts still await the rigorous testing needed for a characterization of novel TTP targets (e.g., 3' UTR reporter assays, physical interaction with TTP etc.), the results demonstrate that 1/3 of unstable mRNAs induced during the acute phase of the innate immune response is destabilized in a TTP-dependent way, and hence are putative TTP targets.

TTP binds to AREs with preference for the UUAUUUUU nonamer in which the positions 1, 2, 8 and 9 can be to some extent occupied with other nucleotides, particularly A (Worthington *et al*, 2002). TTP binding to the AUUUU pentamer, albeit with low affinity, was also demonstrated (Worthington *et al*, 2002). The preferential binding of TTP to such sequences was also confirmed in a genome-wide screen

for mRNA bound to TTP (Lai *et al*, 2006; Emmons *et al*, 2008; Stoecklin *et al*, 2008). In our data set (Supplementary Table 2), the TTP-destabilized LPS-induced transcripts were significantly (***) enriched in AUUUA pentamers ($P=0.0074$) and WWAUUUAWW nonamers ($P=0.0013$) if compared with unstable transcripts not targeted by TTP. This distribution further confirms the dominant role of AREs in TTP-mediated mRNA degradation.

Timing of TTP-dependent degradation of individual mRNAs is controlled by the profile of p38 MAPK activity during inflammatory response

We explain this so far underestimated extent of TTP-dependent mRNA decay by the rapid pharmacological inhibition of p38 MAPK at the peak of inflammatory response, i.e., at the time of still high abundance of inflammatory transcripts. Normally, the p38 MAPK inactivation occurs gradually (Supplementary Figure 3) due to the endogenous IL-10 production that is needed for a sustained expression of *Dusp1* in LPS-treated BMDMs (Hammer *et al*, 2005, 2006; Schaljo *et al*, 2009). Consequently, the TTP-dependent mRNA decay should become more pronounced during the resolution phase of inflammation when the p38 MAPK-mediated inhibition of TTP activity is already strongly diminished. We tested this model by assaying the decay of *Cxcl2* mRNA prior and during the entire inflammatory response to LPS (Figure 2C). Before LPS treatment, *Cxcl2* mRNA was considerably more unstable in WT ($t_{1/2}=49$ min) than in TTP^{-/-} cells ($t_{1/2}=158$ min) showing that the basal amount of TTP present in the cells under low p38 MAPK activity conditions (Supplementary Figure 3) was sufficient to measurably destabilize mRNA. After 3 h treatment with LPS, i.e., under conditions of high p38 MAPK activity (Supplementary Figure 3), *Cxcl2* mRNA was stable in WT cells (Figure 2C) indicating that TTP activity toward *Cxcl2* mRNA was blocked. However, after 6 and 8 h of LPS treatment, i.e., under conditions of diminishing p38 MAPK activity, *Cxcl2* mRNA became gradually unstable in WT cells, and it was more stable in TTP^{-/-} cells at both time points (Figure 2C). The half-lives in WT cells were 68 min at 6 h and 47 min at 8 h whereas in TTP^{-/-} cells the mRNA was stable at 6 h and displayed a half-life of 103 min at 8 h of LPS treatment. The mRNA stability profile demonstrated that *Cxcl2* mRNA was more resistant to TTP-mediated destabilization than, e.g., *Tnf* mRNA since after 3 h of LPS treatment only strong activation of TTP by means of pharmacological inhibition of p38 MAPK revealed the effect of TTP (Figures 1A and 2C), whereas *Tnf* mRNA was destabilized without p38 MAPK inhibition although enhanced destabilization in the presence of the p38 MAPK inhibitor was also observed (Supplementary Figure 4). Together, these data indicate that after the peak p38 MAPK activation and the highest mRNA stabilization the steadily decreasing p38 MAPK activity reduces TTP protein levels but progressively increases TTP activity such that the initially stable TTP targets become destabilized with time. This model is further supported by experiments employing cells and animals with myeloid-specific conditional TTP ablation as described below (Figure 4A; Supplementary Figure 5). The continuous inverse coupling of p38 MAPK activity with the mRNA-destabilizing

function of TTP during the inflammatory response represents an efficient and self-limiting regulatory system that determines the chronology of the elimination of individual mRNAs.

mRNA decay in macrophages with conditional TTP deletion

To validate the proposed regulatory circuit *in vivo* and to circumvent the systemic inflammatory disease of the conventional TTP deletion (Taylor *et al*, 1996), we generated mice lacking TTP in monocytes, macrophages and neutrophils. These cells are the main cell types involved in the lethal outcome of LPS-induced endotoxin shock (Grivennikov *et al*, 2005). Mice for conditional TTP deletion were produced by standard gene-targeting techniques (Figure 3A). Mice bearing loxP-flanked TTP were crossed with LysMcre mice to obtain TTP deletion in myeloid cells (TTP^{ΔM}; Clausen *et al*, 1999). Genomic PCR of BMDMs from TTP^{ΔM} mice indicated successful TTP deletion (Figure 3B). LPS-treated BMDMs obtained from TTP^{ΔM} did not express TTP and produced two-fold more TNF cytokine compared with TTP^{fl/fl} control cells (Figure 3C and D). The induction of *Tnf* mRNA by LPS was similar in TTP^{ΔM} BMDMs and the conventional TTP knockout cells (Taylor *et al*, 1996) further confirming the TTP deficiency in the conditionally ablated cells (Figure 3E).

We used TTP^{ΔM} BMDMs to provide additional evidence for our model describing how a permanent link between p38 MAPK and TTP controls the timing and extent of degradation of individual mRNAs. We analyzed the mRNA stability profile of *Tnf*, the best-known TTP target, *Il1a* as one of the TTP targets identified and characterized in detail in this study, and *Il6* that was recently identified as a target strongly regulated by p38 MAPK (Tudor *et al*, 2009; Zhao *et al*, 2011) at 0, 3, 6 and 9 h of LPS treatment in TTP^{ΔM} and the control TTP^{fl/fl} BMDMs. In TTP^{fl/fl} cells, the initially highly unstable *Tnf* mRNA was stabilized at 3 h after which it became again more unstable: $t_{1/2}=30$ min (LPS 0 h), $t_{1/2}=47$ min (LPS 3 h), $t_{1/2}=20$ min (LPS 6 h) and $t_{1/2}=18$ (LPS 9 h) (Figure 4A). In TTP^{ΔM} cells, *Tnf* mRNA was at all time points more stable compared with the TTP^{fl/fl} control cells: 0 h $t_{1/2}=36$ min (LPS 0 h), $t_{1/2}=180$ min (LPS 3 h), $t_{1/2}=69$ min (LPS 6 h) and $t_{1/2}=53$ min (LPS 9 h) (Figure 4A). Thus, in contrast to *Cxcl2* mRNA (Figure 2C), TTP was able to destabilize *Tnf* also at high p38 MAPK activity confirming previous reports and above-mentioned data (Supplementary Figure 4). However, similar to *Cxcl2*, TTP exhibited increasing destabilizing activity toward *Tnf* mRNA at later time points as apparent from the ratios of remaining mRNA amounts in TTP^{ΔM} cells versus TTP^{fl/fl} cells (Figure 4B). *Il1a* and *Il6* mRNAs were generally more stable throughout the time course, but both displayed decreased stability at 6 h (for *Il1a*) and 9 h (for both *Il1a* and *Il6*) in TTP^{fl/fl} cells whereas in TTP^{ΔM} they remained stable (*Il1a* throughout the time course, *Il6* for 3 and 6 h) or were only slightly destabilized (*Il6* for 9 h) (Supplementary Figure 5). Due to low expression of these two cytokines in unstimulated cells, we were not able to obtain consistent results at 0 h. Together, these experiments supported our model derived from the analysis of the *Cxcl2* mRNA stability profile (Figure 2) that early after LPS stimulation the TTP-dependent mRNA decay is inhibited, but

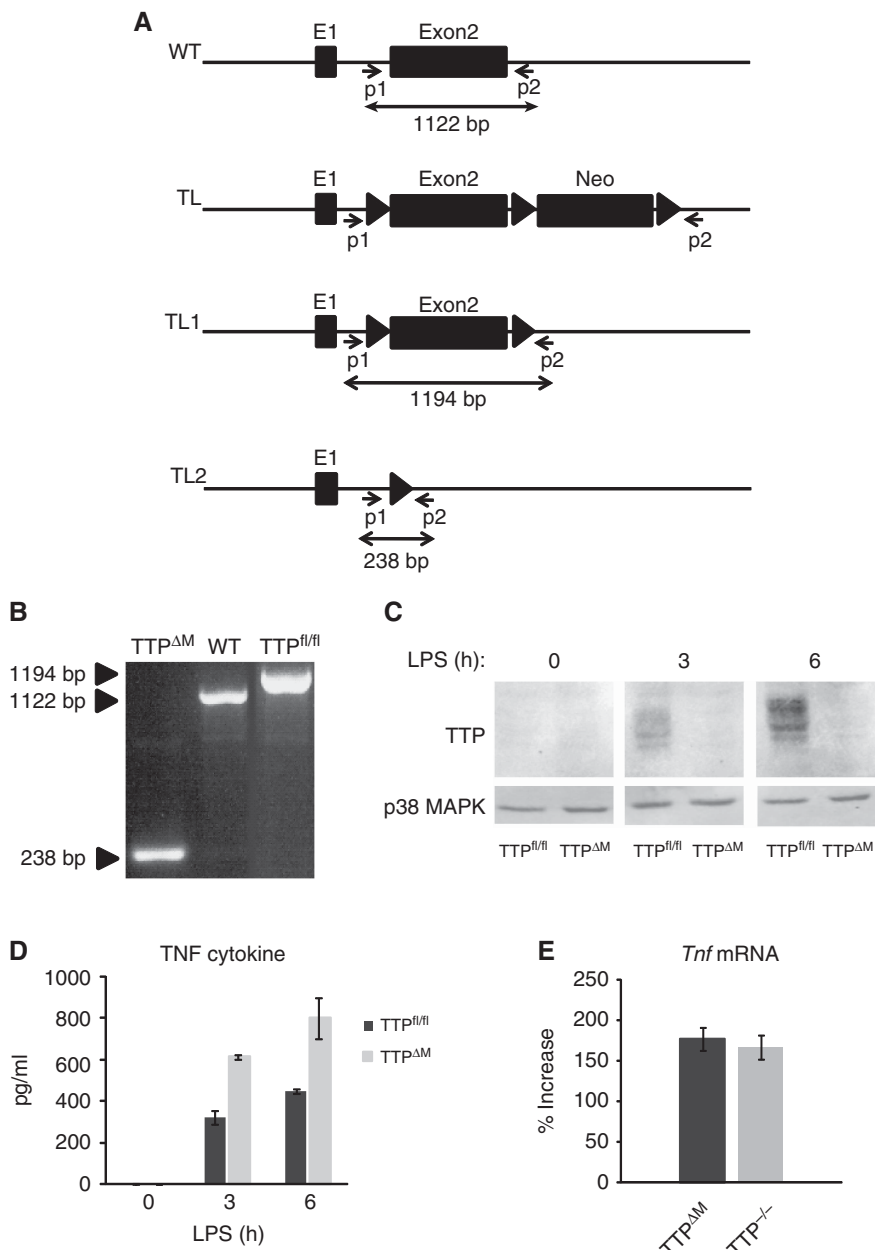


Figure 3 Generation of TTP^{fl/fl} mice and analysis of functional TTP deletion in BMDMs derived from TTP^{ΔM} mice. **(A)** Scheme of targeting strategy in the TTP (*Zfp36*) locus. WT: wild-type TTP locus; TL: targeted TTP locus; triangles: loxP sites; TL1: targeted locus after Cre-mediated excision of the Neo cassette; TL2: targeted locus after Cre-mediated excision of exon 2 of TTP; E1=exon 1; p1 and p2=primers used for the detection of Cre-mediated deletion in **(B)**. Expected PCR fragment size is indicated. **(B)** PCR of genomic DNA isolated from BMDMs derived from the respective mice. The size of PCR products corresponds to the expected size depicted in **(A)**. **(C)** Western blot analysis of whole cell extracts of BMDMs derived from TTP^{fl/fl} and TTP^{ΔM} mice. BMDMs were stimulated with LPS for 3 or 6 h or left untreated. TTP expression was examined using TTP antibody. The membrane was re-probed with antibody to p38 MAPK for loading control. **(D)** BMDMs from TTP^{ΔM} mice produce two-fold more TNF cytokine compared with control cells from TTP^{fl/fl} littermates (determined in supernatants of cells treated for 3 and 6 h with LPS). Error bars display s.e.m. ($n=3$). **(E)** Induction of *Tnf* mRNA by LPS in BMDMs from TTP^{ΔM} mice and conventional TTP knockout mice (TTP^{-/-}) is comparable (determined by qRT-PCR after treatment of cells for 3 h with LPS). Error bars display s.e.m. ($n=3$). Source data is available for this figure in the Supplementary Information.

thereafter it progressively unfolds in terms of quality and quantity. Analysis of *Tnf* mRNA decay further revealed that in unstimulated cells (0 h LPS) the *Tnf* mRNA was unstable also in TTP^{ΔM} cells although it was still even more unstable in TTP^{fl/fl} cells ($t_{1/2}=36$ min in TTP^{ΔM} versus $t_{1/2}=30$ min in TTP^{fl/fl}) (Figure 4A). The TTP-independent *Tnf* mRNA degradation was abolished or reduced after 3 and 6 h of LPS

treatment since the *Tnf* message was stabilized in TTP^{ΔM} cells at these time points (Figure 4A). After 9 h of LPS treatment, the TTP-independent component of *Tnf* mRNA degradation became apparent again, although to a lesser extent than at 0 h (Figure 4A). *Tnf* mRNA can be destabilized by other members of the TTP family, the Tis11b and Tis11c proteins (gene names *Zfp36l1* and *Zfp36l2*, respectively) although the

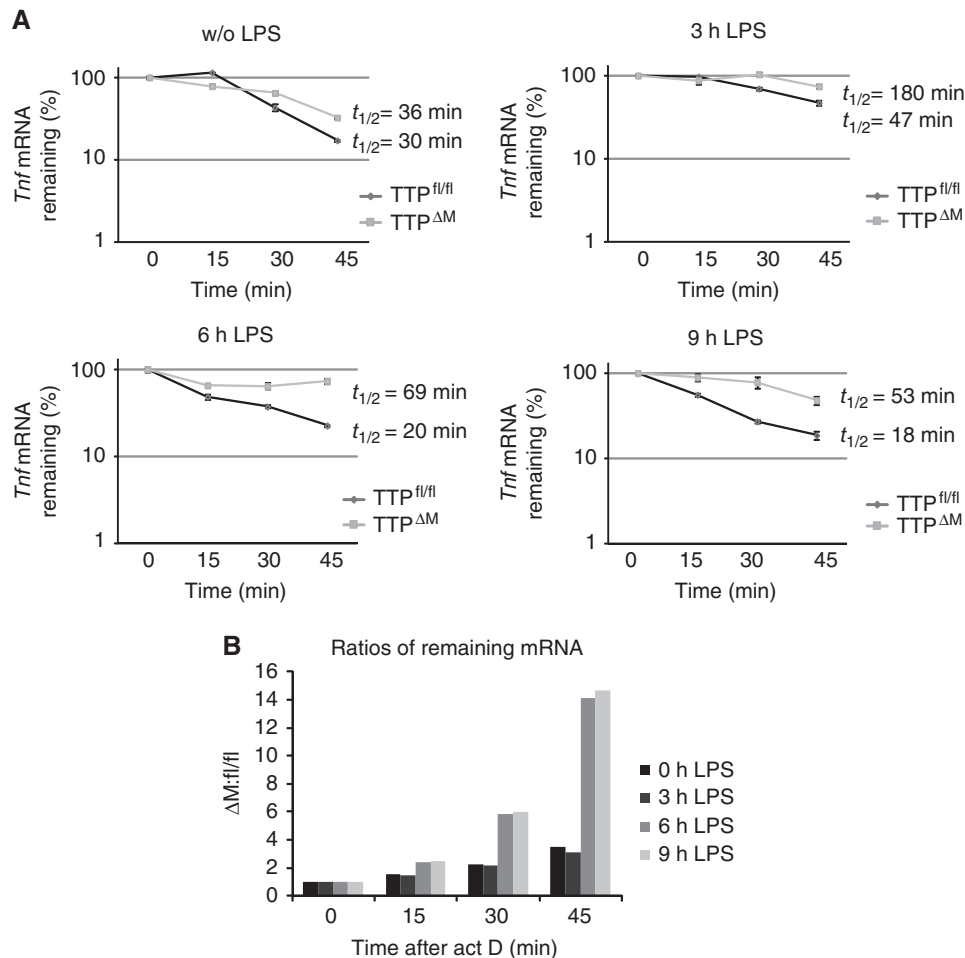


Figure 4 *Tnf* mRNA stability profile during LPS response. *Tnf* mRNA becomes progressively destabilized in a TTP-dependent manner after prolonged LPS treatment. TTP^{ΔM} and control TTP^{fl/fl} BMDMs were left untreated or were stimulated for 3, 6 or 9 h with LPS followed by transcriptional blockage with act D for indicated times. **(A)** Decay rate of *Tnf* was monitored by qRT-PCR. Remnant *Cxcl2* mRNA in percent of the amount at the time point of act D treatment is depicted; s.e.m. is shown ($n=3$). **(B)** Ratios of remaining *Tnf* mRNA in TTP^{ΔM} versus TTP^{fl/fl} cells calculated from the half-lives shown in (A) are depicted. Source data is available for this figure in the Supplementary Information.

regulation of mRNA degradation by these proteins and their targets *in vivo* are poorly understood (Lai *et al*, 2000; Hodson *et al*, 2010). We noticed that expression of Tis11b and Tis11c was high in unstimulated cells but it rapidly dropped after LPS stimulation (Supplementary Figure 6). This expression profile suggested that the TTP-independent *Tnf* mRNA degradation before LPS stimulation could be caused by Tis11b and Tis11c. The rapid decrease of Tis11b and Tis11c expression after LPS treatment was consistent with the disappearance of the TTP-independent *Tnf* mRNA decay.

The TTP-dependent *Tnf* mRNA destabilization in unstimulated cells (Figure 4A) resembled the observation obtained for *Cxcl2* (Figure 2C), and it further confirmed that the basal TTP expression was sufficient to measurably destabilize TTP targets. TTP expression was low but detectable at both mRNA and protein levels in unstimulated cells (Supplementary Figure 7). Regardless of the mRNA degradation by TTP in cells before LPS treatment, the mRNA stability profile of *Tnf*, *Il1a* and *Il6* at 3, 6 and 9 h after LPS treatment was in agreement with the model of gradually increasing TTP activity as first revealed by analysis of *Cxcl2* (Figure 2C). To substantiate our model, we

employed microarrays to analyze mRNA stability at 3 and 9 h after LPS stimulation of TTP^{fl/fl} and TTP^{ΔM} BMDMs. mRNA amounts were determined before (0 min) and 90 min after the transcription inhibition by act D. We calculated half-lives of novel TTP targets for which we show RNA immunoprecipitation data in Figure 1D (*Ccl2*, *Ccl4*, *Ccl7*, *Cxcl2*, *Ets2*, *Il1a*, *Junb*, *Plaur* and *Tnfsf9*), as well as for targets identified in previous screens (*Ccl3*, *Cxcl1*, *Ier3*, *Il6*, *Il10*, *Il12b* and *Tnf*). Averaged log₂-transformed microarray signal intensities derived from three biological replicates for each of these genes (Supplementary Table 3) were used for half-life calculations. As shown in Table III, except for *Ccl2*, *Junb* and *Ets2* all targets displayed half-lives that were in agreement with the proposed model since the mRNAs were less stable after 9 h LPS than after 3 h LPS in TTP^{fl/fl} cells, and at the same time they were always more stable in TTP^{ΔM} cells. Importantly, in most cases the half-life differences between TTP^{fl/fl} and TTP^{ΔM} cells confirmed progressively increasing TTP-dependent mRNA degradation with time of LPS treatment. *Ccl2* was stable under these conditions (in contrast to experiments employing p38 MAPK inhibition in Table II), suggesting that p38 MAPK was still too

Table III Decay rates in TTP^{ΔM} and TTP^{fl/fl} BMDMs at 3 and 9 h of LPS treatment

Nr.	RNA accession nr.	Gene name	3 h LPS, TTP ^{fl/fl} half-life (min)	3 h LPS, TTP ^{ΔM} half-life (min)	9 h LPS, TTP ^{fl/fl} half-life (min)	9 h LPS, TTP ^{ΔM} half-life (min)
1	NM_011333	<i>Ccl2</i>	Stable	Stable	Stable	Stable
2	NM_011337	<i>Ccl3</i>	Stable	Stable	58	Stable
3	NM_013652	<i>Ccl4</i>	541	Stable	31	41
4	NM_013654	<i>Ccl7</i>	Stable	Stable	486	Stable
5	NM_008176	<i>Cxcl1</i>	104	202	19	30
6	NM_009140	<i>Cxcl2</i>	Stable	Stable	39	84
7	NM_011809	<i>Ets2</i>	68	73	107	107
8	NM_133662	<i>Ier3</i>	36	79	12	17
9	NM_010548	<i>Il10</i>	Stable	Stable	70	226
10	NM_010554	<i>Il1a</i>	Stable	Stable	29	197
11	NM_008361	<i>Il1b</i>	Stable	Stable	49	174
12	NM_031168	<i>Il6</i>	Stable	152	44	111
13	NM_008416	<i>Junb</i>	25	30	19	17
14	NM_011113	<i>Plaur</i>	Stable	Stable	118	541
15	NM_013693	<i>Tnf</i>	54	283	12	23
16	NM_009404	<i>Tnfsf9</i>	26	35	20	28

high to allow *Ccl2* mRNA degradation. *Junb* and *Ets2* were more stable in TTP^{ΔM} BMDMs than in TTP^{fl/fl} only after 3 h of LPS treatment but not after 9 h, suggesting that TTP-independent decay mechanisms became more prominent for these targets at later phase of LPS stimulation. Cumulatively, the mRNA stability profiles obtained using different approaches supported the proposed model for the regulation of timing and extent of mRNA decay by TTP.

Ablation of TTP in myeloid cells is not detrimental to health but causes hypersensitivity to LPS and dysregulated timing of cytokine production

For validation of our model of TTP-mediated mRNA decay, we employed LPS-induced shock. At the age of 6–12 weeks, i.e., the age at which animals were used for experiments, TTP^{ΔM} mice appeared healthy, had normal body weight (Figure 5A) and were fertile. No aberrant blood counts and no signs of dermatitis were detected (Figure 5B and C). TTP^{ΔM} animals remained free of dermatitis and cachexia until the age of at least 7 months, the latest time of observation, when most of the conventional TTP^{-/-} mice on the same background (C57BL/6) and in the same animal facility developed severe inflammation or had already died from it (unpublished observation). These data implicate that cells other than those with LysMcre-mediated TTP deletion (e.g., dendritic cells) or macrophages resistant to LysMcre function contributed to the chronic inflammation and infertility observed in the conventional TTP knockout mice (Taylor *et al*, 1996). Similarly to the conventional TTP knockout mice, a modest splenomegaly was observed in the TTP^{ΔM} animals (Figure 5D). Lethal LPS challenge of the TTP^{ΔM} mice revealed increased susceptibility compared with the TTP^{fl/fl} control littermates (Figure 6A). TTP^{ΔM} mice exhibited elevated serum levels of the proinflammatory TNF, Cxcl1 and Cxcl2 as well as the anti-inflammatory IL-10 after LPS challenge. All these cytokines and chemokines were below the detection level before LPS challenge in both genotypes (unpublished observation). The difference in TNF levels was apparent already after 1 h of LPS treatment whereas the difference in IL-10 was detectable after

3 h (Figure 6B). The profiles of Cxcl1 and Cxcl2 displayed the highest difference after 8 h of LPS treatment (Figure 6C). These data are in agreement with the profile of mRNA stability in WT versus TTP^{-/-} or TTP^{fl/fl} versus TTP^{ΔM} macrophages showing TTP effect on *Tnf* mRNA at the peak of inflammatory response, whereas the effect on *Cxcl2* was detectable either only upon p38 MAPK inhibition or at the later phase of inflammation when p38 MAPK activity dropped (Figures 4A and 2C, respectively). Similarly, *Cxcl1* mRNA was found strongly destabilized in WT macrophages only upon inhibition of p38 MAPK (Datta *et al*, 2008) or at the later time point after LPS stimulation (Table III). These data demonstrate the functional importance of the TTP-mediated control of timing and quality of mRNA decay for the regulation of inflammatory mediators *in vivo*. This control allows sequential shut-off of individual cytokines such that potentially deleterious effects of a premature or delayed termination of these cytokines are prevented. The LPS endotoxin shock model reveals that myeloid TTP is phenotypically more important in the control of the proinflammatory factors since the higher IL-10 levels in the TTP^{ΔM} mice were not able to reverse the increased sensitivity to LPS. The overall good health of TTP^{ΔM} animals together with their increased susceptibility to LPS indicates that myeloid TTP is not primarily involved in the maintenance of immune homeostasis under steady-state conditions but rather controls balanced responses to inflammatory stimuli such as TLR ligation.

Discussion

Cessation of transcription does not immediately result in the termination of expression unless the already generated mRNAs are degraded. This has been demonstrated by studies describing lethal consequences of uncontrolled *Tnf* expression caused by the removal of AREs from its 3' UTR (Kontoyiannis *et al*, 1999; Murray, 2005). On the other hand, immune cells must be able to robustly stimulate the expression of inflammatory genes in the early phase of the inflammatory response. In addition, the shutdown of the most potent inflammatory cytokines (e.g., *Tnf*) must precede the down-

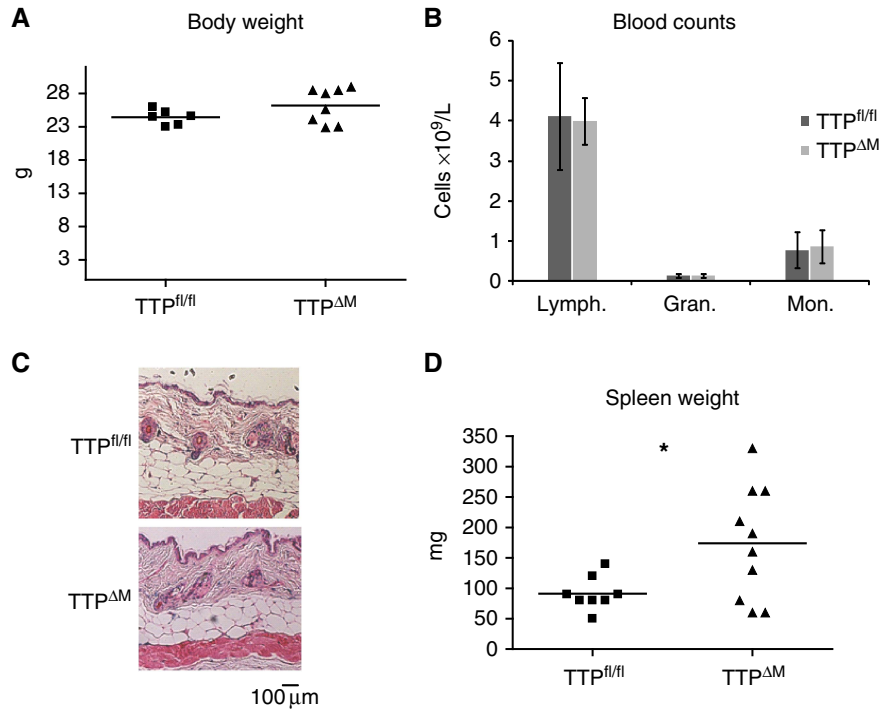


Figure 5 TTP ΔM mice are healthy. **(A)** Sex-matched (males) TTP ΔM mice ($n=8$) and control TTP $^{fl/fl}$ littermates ($n=6$) have comparable body weight (age of both genotypes: 9 weeks). **(B)** Sex-matched (females) TTP ΔM mice ($n=3$) and control TTP $^{fl/fl}$ littermates ($n=5$) have normal blood counts (age of both genotypes: 6–8 weeks). **(C)** Skin of female TTP ΔM mice and control TTP $^{fl/fl}$ littermates displays healthy architecture with comparable subcutaneous fat tissue and no signs of dermatitis (H&E-stained sections representative of at least five 7–9-week-old animals are shown). **(D)** Spleen of TTP ΔM mice ($n=10$) exhibit 70% increased weight compared with control TTP $^{fl/fl}$ littermates ($n=8$). Animals of both genotypes were males of 9–10 weeks of age. Significance of different spleen weight is indicated by asterisk ($*P < 0.05$). Source data is available for this figure in the Supplementary Information.

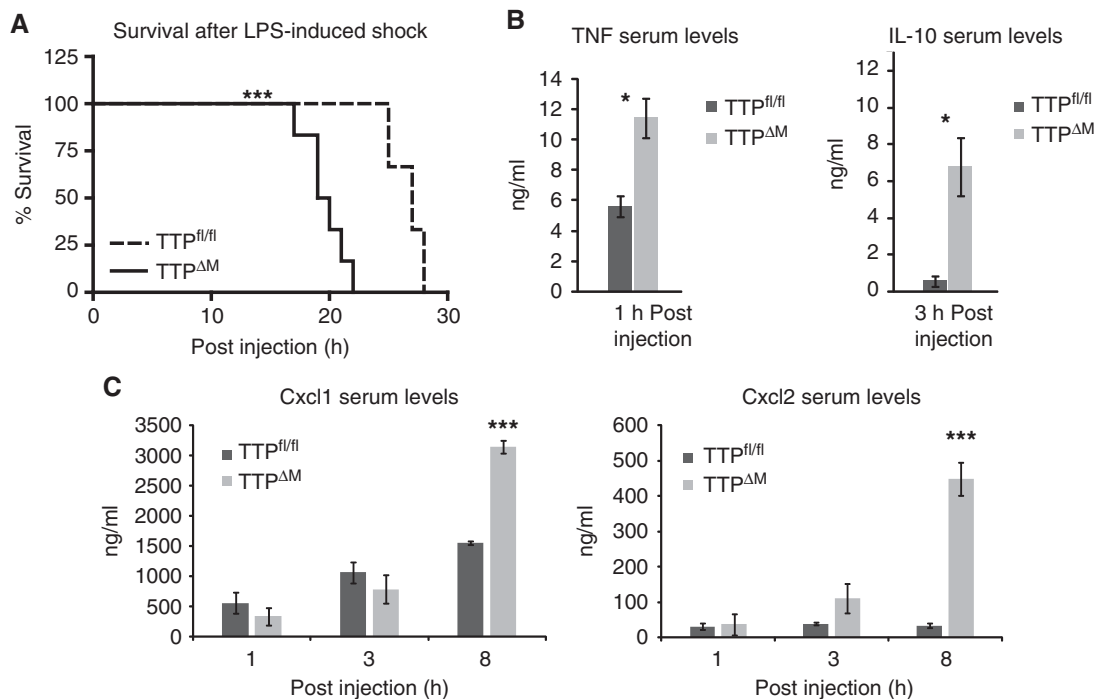


Figure 6 TTP ΔM mice are more susceptible to LPS-induced endotoxin shock and exhibit dysregulated temporal control of cytokine production. **(A)** Kaplan–Meier survival curves reveal increased lethality of female TTP ΔM mice ($n=6$) compared with control TTP $^{fl/fl}$ littermates ($n=6$) after LPS challenge. Animals of both genotypes were females of 9–10 weeks of age. Experiments were carried out three times with similar outcome. **(B)** TTP ΔM mice exhibit elevated serum levels of TNF (after 1 h of LPS treatment) and IL-10 (after 3 h of LPS treatment) compared with control TTP $^{fl/fl}$ littermates. **(C)** Cxcl1 and Cxcl2 levels were increased only at later time points after LPS treatment in the serum of TTP ΔM mice compared with TTP $^{fl/fl}$ littermates. In **(B)** and **(C)**, error bars display s.e.m. ($n=5$); significance of different cytokine levels is indicated by asterisks. Source data is available for this figure in the Supplementary Information.

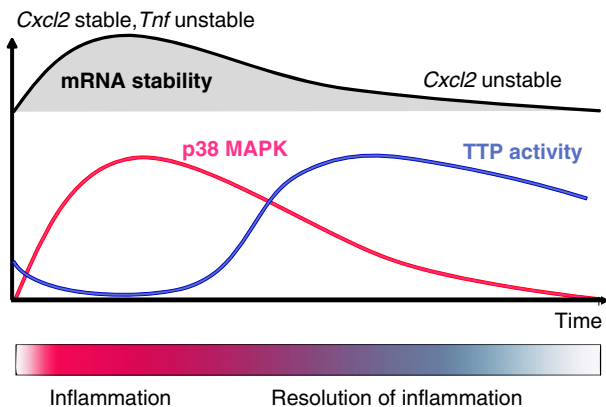


Figure 7 Scheme of the qualitative and temporal control of inflammatory mRNA decay by the p38 MAPK/TTP-dominated circuit. Inflammatory stimulus activates the stress-regulated p38 MAPK that in turn inhibits the mRNA-destabilizing function of TTP. In this phase, TTP destabilizes only few mRNAs (e.g., *Tnf*). The mRNA-destabilizing function of TTP progressively unfolds and spreads to more mRNAs (e.g., *Cxcl2*) as a consequence of continuous decrease of p38 MAPK activity.

regulation of anti-inflammatory (e.g., *Il10*) or tissue-regenerating cytokines. Thus, a mechanism must be in place that attenuates the inflammatory mRNA degradation with some delay after the initial inflammatory stimulus. The delay is variable but specific for individual mRNAs. This study describes a TTP- and p38 MAPK-driven negative feedback system that executes a delayed yet robust elimination of a large number of inflammation-induced mRNAs in a qualitative and temporally resolved manner (Figure 7). The downstream effector of the system is the ARE-binding protein TTP whose mRNA-destabilizing function inversely correlates with the profile of p38 MAPK activity during the entire inflammatory response. This negative regulatory circuit is operational also *in vivo* since its inactivation impairs the ability of mice to cope with inflammatory challenge but the mice are still able to maintain their immune homeostasis under steady-state conditions.

The large extent of TTP-dependent mRNA decay uncovered by the microarray-based differential analysis of mRNA stability is supported by several lines of evidence. First, we employed the most stringent criterion for finding TTP targets namely a slower decay in $TTP^{-/-}$ compared with WT cells instead just increased steady-state mRNA levels in $TTP^{-/-}$ cells or a direct physical interaction of mRNA with TTP. Second, two selected mRNAs were confirmed by detailed studies as TTP targets. Third, all the best-characterized TTP targets expressed in macrophages were identified as TTP targets in our profile as well. Fourth, the TTP-destabilized mRNAs were enriched in the WWAUUUAWW nonamers, which are AREs with high affinity for TTP. Fifth, we show direct association of seven additional TTP-destabilized ARE-containing mRNAs (*Ccl2*, *Ccl4*, *Ccl7*, *Ets2*, *Junb*, *Plaur* and *Trnfsf9*) with TTP. The large number of TTP targets in our data set resulted from increased sensitivity of the analysis due to an abrupt inhibition of p38 MAPK at the time of still high presence of inflammatory mRNAs. The pharmacological p38 MAPK inhibition did not introduce an artificial TTP-dependent decay but rather revealed the upper limit of TTP targets. This

is documented by the mRNA stability profile of *Cxcl2* displaying increasing TTP-dependent decay following the spontaneous drop of p38 MAPK activity. In further support, *fos* mRNA that is known to be unstable independently of TTP (Stoecklin *et al*, 2001; Lai *et al*, 2006) was unstable yet not targeted by TTP in our study as well. For all these reasons, we conclude that the majority of mRNAs stabilized in $TTP^{-/-}$ cells are direct TTP targets. Nevertheless, indirect effects of TTP by, e.g., upregulation of an inhibitor of mRNA decay in $TTP^{-/-}$ cells cannot be entirely ruled out as demonstrated by the presence of the few ARE-free mRNAs in our data set. However, the mRNA levels of HuR, the most prominent mRNA-stabilizing factor that in some cases antagonizes TTP (Abdelmohsen *et al*, 2007), were comparable in WT and $TTP^{-/-}$ cells in the microarray data set (<http://www.ncbi.nlm.nih.gov/geo/>, accession number GSE28880).

Our study indicates that the TTP-mediated mRNA destabilization process discriminates between the different targets depending on the p38 MAPK activity. This allows for a fine-tuning of the control of the inflammatory response in terms of both kinetics and strength. Whereas some targets can be significantly degraded also at a high p38 MAPK activity (e.g., *Tnf*), for the decay of other targets a low p38 MAPK activity, i.e., a high TTP activity is needed. This is illustrated by the high stability of *Cxcl2* after 3 h of LPS treatment when only an inhibition of p38 MAPK reveals this target to be unstable. After 6 and 8 h of LPS treatment, *Cxcl2* becomes spontaneously unstable and the inhibition of p38 MAPK is no longer needed to detect TTP-dependent decay. This temporal and qualitative control of mRNA decay by TTP is observed also *in vivo* since mice with TTP ablation in macrophages display sequential increase of several cytokines upon LPS challenge compared with WT animals. How does p38 MAPK enable TTP to discriminate between different targets is an important topic for future studies. The sequence of the ARE alone cannot account for the observed differences since both *Tnf* and *Cxcl2* possess comparable AREs yet only *Tnf* is destabilized by TTP at a high p38 MAPK activity. Thus, so far unknown regulatory elements in the 3' UTRs such as micro RNA-binding sites are likely to be involved (von Roretz and Gallouzi, 2008). Another aspect of the integrated regulation of mRNA decay was revealed by our experiments in unstimulated cells showing that *Tnf* mRNA was significantly destabilized also independently of TTP whereas *Cxcl2* mRNA was only slightly unstable in the absence of TTP. The TTP-independent *Tnf* mRNA decay was almost abolished upon LPS treatment. Since expression of the TTP-related proteins Tis11b and Tis11c was inhibited by LPS, it is intriguing to speculate that these proteins might be targeting *Tnf* together with TTP under steady-state conditions whereas TTP alone is the major *Tnf* mRNA-destabilizing factor during inflammation. The advantage of such a system lies in the regulation of TTP activity by the continuous inverse coupling to p38 MAPK that allows permanent sensing of the inflammatory status. Such regulation has so far not been reported for Tis11b and Tis11c. One could hypothesize that the small extent of TTP-independent decay of *Cxcl2* mRNA compared with *Tnf* mRNA in unstimulated cells is caused by differential target specificity of Tis11b and Tis11c toward these transcripts. Given the currently limited knowledge about Tis11b and Tis11c with regard to their regulation and targets

in vivo, more comprehensive studies of these proteins will be required in the future to establish functional links within the TTP protein family.

Despite the ability of TTP to profoundly control gene expression in macrophages, the phenotypic effects were restricted on broad feedback control after inflammatory challenge demonstrating the remarkable specificity of the TTP function. Mice with LysMcre-driven deletion of TTP did not display the multiple inflammatory pathologies of the conventional TTP knockout except of splenomegaly (Taylor *et al*, 1996). This finding indicates that the complex hyperinflammation seen in the complete TTP knockout is caused primarily by cells other than macrophages and granulocytes since LysMcre deletes in these cell types (Clausen *et al*, 1999). In addition, the good health of the conditionally deleted mice and the LPS hypersensitivity demonstrate that myeloid TTP is required for the dampening of gene expression after an inflammatory stimulus rather than for a continuous monitoring of the immune homeostasis under steady-state conditions. In further support, the increased cytokine levels in the serum of TTP^{ΔM} mice relative to TTP^{fl/fl} controls were observed after LPS challenge but not before it. The inability of elevated IL-10 levels in TTP^{ΔM} mice to compensate the high TNF and other inflammatory mediators in the endotoxin shock model was not surprising since the most beneficial anti-inflammatory effects of IL-10 are observed only if animals are exposed to IL-10 before the LPS challenge (Berg *et al*, 1995). Furthermore, IL-10 cannot unfold its full activity in the TTP^{ΔM} animals since TTP is one of its downstream effectors (Schaljo *et al*, 2009).

Our study provides insight into the temporal and qualitative control of acute inflammation *in vivo*. The data explain how the control of mRNA stability contributes to the chronologically restricted function of individual inflammatory mediators in certain phases of the acute inflammatory response. The underlying regulatory circuit consisting of p38 MAPK and TTP has an outstanding functional specificity for inflammatory processes as shown by our animal studies. This characteristic is so far unique among the best-characterized ARE-binding proteins such as the TTP homologs TIS11b and TIS11d, or the RNA-stabilizing HuR which appear to have more pleiotropic functions (Ghosh *et al*, 2009; Hodson *et al*, 2010). The tight inverse coupling of TTP function with p38 MAPK activity and the self-regulatory features (e.g., disappearance of TTP expression with the drop of p38 MAPK activity) may in part explain the functional specificity of this control system. This regulatory circuit is likely to have co-evolved with the immune system since *Drosophila* may employ similar mechanisms to control inflammation (Cairrao *et al*, 2009) whereas yeast does not appear to have such coupled regulation although the individual players such as p38 MAPK, ARE-binding proteins and ARE-mediated mRNA decay are present (Puig *et al*, 2005).

Materials and methods

Microarray analysis of mRNA decay (with p38 MAPK inhibitor SB203580)

BMDMs from WT and TTP^{-/-} mice were treated with LPS for 3 h. Medium was then replaced by fresh medium containing act D and SB203580 for 0, 45 and 90 min before RNA extraction. BMDMs from three different mice were used for each time point, i.e., in total 18

independent biological samples were collected (9 for WT and 9 for TTP^{-/-} cells). Total RNA was then used for genome-wide expression analysis using Affymetrix Mouse Gene ST 1.0 microarrays containing 28 853 genes. Standard protocols for labeling and hybridization were followed. In brief, 200 ng of total RNA was reverse transcribed introducing by random priming a T7-binding site into the cDNA for subsequent *in-vitro* transcription. The resulting cRNA was subjected to a second round of random primed cDNA synthesis in the presence of dUTP, which allows fragmentation of the cDNA with uracil DNA glycosylase and apurinic/apyrimidinic endonuclease 1. Fragmented cDNA was biotinylated by incubation with terminal deoxynucleotidyltransferase (TdT), and 5.5 μg of biotinylated DNA was hybridized to Mouse Gene ST 1.0 GeneChips overnight, washed, stained and scanned following Affymetrix protocols. For generation of probe set expression values, CEL files containing probe level data were normalized using the RMA algorithm implemented in the Affymetrix Expression Console. Microarray data have been deposited in Gene Expression Omnibus (GEO, <http://www.ncbi.nlm.nih.gov/geo/>), accession number GSE28880. Subsequently, the data were log-transformed, after subtraction of a constant of 1.41 to account for the background, to achieve approximate normality and standardized to zero mean and unit variance. A linear model with genotype (WT and TTP^{-/-}), treatment (0, 45 and 90 min) and their interaction as independent variables was fitted. Residual variances were adjusted using an empirical Bayes method (Smyth, 2004) to obtain approximately *t*-distributed differences in gene expression values. It turned out that the resulting distribution of log 2-transformed signal intensities was slightly bi-modal, with a sharp peak at low values. We interpreted this peak as resulting from spurious background fluorescence of unexpressed genes. Thus, we filtered out genes expressed at an absolute level of <11.3, which falls into the valley between the two peaks. In addition, many fewer genes could be classified as unstable at the 45-min decay time point (due to the lower difference in relation to the variation at this time point) than at 90 min so that only the results for the 90-min time point are presented. The most extremely regulated genes were then selected according to the following criteria: (i) genes where the decay of mRNAs after 90 min was outside the one-sided $\alpha=0.05$ limit (=one *; or $P<0.05$) (t -value > 1.86); (ii) genes where additionally the decay of mRNAs in TTP^{-/-} compared with WT cells after 90 min was outside the one-sided $\alpha=0.05$ limit.

The half-lives were determined using the microarray data set. First, the average difference between the time point 0 min (=transcription blockage) and 90 min (end of the decay assay) in the three biological replicates was calculated for each mRNA. These average decay values were then used to calculate the half-lives assuming an exponential decay. For half-lives > 600 min, the value was set as 'stable'. For direct access and to allow comparison with other global screens for TTP targets, the data set is deposited in the AREsite (<http://rna.tbi.univie.ac.at/cgi-bin/AREsite.cgi>) (Gruber *et al*, 2011) (available after acceptance of the paper).

Analysis of mRNA decay in the LPS-induced transcriptome

LPS-induced genes were retrieved from our recently published microarray data set (GEO accession number GSE8621; Mages *et al*, 2007) obtained by stimulation of BMDMs for 3 h with LPS. Transcripts that were induced at least three-fold in comparison with unstimulated cells were examined with regard to their decay rates using the mRNA decay data set from this study.

Construction of TTP targeting vector and generation of mice with conditional TTP deletion

For conditional deletion of TTP, the CreLoxP strategy is used. TTP (*Zfp36*) targeting vector was generated by inserting LoxP sites at both sides of exon 2. Homologous integration of the vector after selection using neomycin was monitored by PCR. Before blastocyst injection, the neomycin resistance cassette was excised by transiently transfecting targeted ES cells with a Cre recombinase-expressing construct.

Loss of the Neo cassette but not exon 2 was monitored by PCR using primers p1 and p2 that were also used for subsequent genotyping (Figure 3A). Two positive clones were injected into C57BL/6 blastocysts and used to generate chimeric mice. Male chimeric mice were mated to C57BL/6 females and heterozygote offspring were further backcrossed five times with C57BL/6 using speed congenics for selection of animals with the highest C57BL/6 background (Wakeland *et al*, 1997). Assessment of 112 genetic markers revealed over 98.8% C57BL/6 background in the animals used for further breeding.

Mice

TTP^{-/-} (*Zfp36*^{-/-}) mice (Taylor *et al*, 1996) were on C57BL/6 background (backcrossed 10 times to C57BL/6). Mice conditionally deleting TTP in myeloid cells were obtained by breeding TTP^{fl/fl} mice to LysMcre mice (Clausen *et al*, 1999) on C57BL/6 background to generate TTP^{fl/fl} bearing single LysMcre allele (=TTP^{ΔM}). All mice were housed under specific pathogen-free conditions. All animal experiments were discussed and approved by the institutional ethics committee and conform with the Austrian law (ref. 68.205/0204-C/GT/2007, ref. 68.205/0233-II/10b/2009 and ref. 66.006/0002-II/10b/2010).

ELISA

For ELISA of serum, blood serum was prepared as described and diluted 1/10. For ELISA of BMDMs, 2 × 10⁵ cells/well were seeded the day before in a 24-well plate. Supernatants were collected and diluted 1/8 before usage. Cytokine concentration of TNF, Cxcl1, Cxcl2 and IL-10 was determined using ELISA kits (R&D Systems).

Blood analysis

Blood counts of peripheral blood were determined using a V-Sight Hematology Analyzer (A. Menarini Diagnostics).

LPS-induced endotoxin shock

Animal experiments were performed with sex- and age-matched (8 weeks) mouse groups (*n*=10) for TTP^{fl/fl} and TTP^{ΔM} mice. LPS at a concentration of 62.5 mg/kg body weight dissolved in 0.9% NaCl was injected intraperitoneally. Mice were then monitored for time of death to calculate a Kaplan–Meier blot. For the calculation of cytokine levels in blood serum, groups of three mice were treated with LPS for 0, 1 or 3 h before withdrawing peripheral blood. The blood was coagulated and then centrifuged at 1000 g for 15 min before collecting the serum.

Quantitation of gene expression by qRT–PCR

Total RNA was isolated using Trizol reagent (Invitrogen) and reverse transcribed by Mu-MLV reverse transcriptase (Fermentas). Amplification of DNA was monitored by SYBR Green (Molecular Probes) as described (Morrison *et al*, 1998). Primers for rabbit β-globin, *Tnf*, *Il6* and murine or human *Hprt* are listed in the primer list. For detection of *Cxcl2*, *Il1b*, *Il1a*, *Il10*, *Tis11b* (gene name *Zfp3611*) and *Tis11c* (gene name *Zfp3612*) QuantiTect Primer Assays (Qiagen) QT00113253, QT01048355, QT00113505, QT00106169, QT00287056 and QT01780975, respectively, were used.

Measurements of mRNA stability

In all, 5 × 10⁶ HeLa Tet-Off cells were transfected by nucleofection with 1 μg pTetBBB/IL1α, pTetBBB/Cxcl2 or pTet/HPRT together with 4 μg pCMV-TTP or 4 μg empty pCMV. Twenty-four hours later, 200 ng/ml tetracycline was added to stop transcription from the pTetBBB plasmids. Total RNA was prepared and analyzed by qRT–PCR as described. To assay mRNA stability in BMDMs, 5 × 10⁶ cells were treated with LPS as indicated in the figure legends. Medium was then removed and fresh medium containing act D and, if appropriate,

SB203580 was added for the times indicated before preparing total RNA. RNA was analyzed by qRT–PCR as described before or used for microarray hybridization.

RNA electrophoretic mobility shift assay

To prepare TTP-containing extracts, HeLa Tet-Off cells were transfected with pTRE-TTPfl plasmid as described (Schaljo *et al*, 2009). Twenty-four hours after transfection, the cells were washed with cold PBS and lysed in buffer containing 10 mM Tris–HCl (pH 7.5), 50 mM NaCl, 30 mM NaPP_i, 50 mM NaF, 2 mM EDTA, 1% Triton X-100 and protease inhibitor cocktail (Roche). Extracts were cleared by centrifugation at 15000 r.p.m. In all, 5 μl cell extract (15 μg protein) was incubated with 0.5 μl Poly-U RNA (100 ng/μl) (Microsynth), 0.5 μl Cy5.5 5′-labeled Tnf ARE (1 pmol/μl), 1 μl RiboLock RNase Inhibitor (Fermentas) and 2.5 μl 5 × gel shift buffer (200 mM KCl, 5 mM MgCl₂, 0.5 mM EGTA, 2.5 mM DTT, 100 mM Hepes–KOH pH 7.9, Glycerin 50% (v/v)) for 20 min at room temperature. For supershift assays, 0.5 μl anti-Flag M2 antibody (Sigma) was added. For competition experiments, 0.5 μl competing RNA oligonucleotides were added at a concentration of 0, 1, 10 or 100 pmol/μl for further 20 min. Samples were then separated on a 6% polyacrylamide gel. The Cy5.5 signal was detected and quantified using the infrared imaging system Odyssey (LI-COR Biosciences). RNA oligonucleotides and the *Tnf* RNA Cy5.5 5′-labeled oligonucleotide were purchased from Microsynth. The RNA sequence was as follows: for Cy5.5 5′-labeled or unlabeled *Tnf* ARE, Cy5-TNFα-ARE 5′-AUUUAUUUUAUUUUAUUUUAUUUUAUUUUA-3′; as random sequence, random 5′-AGCUUAGGAAUAUCAUGUUAAGUAG-3′; for the *Il1a* ARE, *Il1a*-ARE 5′-UAUUUAUAUAUAUUUUAUGAUAAUUAUUAUUUUAU-3′; for the *Cxcl2* ARE, *Cxcl2*-ARE 5′-UUAUUUUAUUUAUUAUGUUAUUUUAUUUUAUUU-3′.

RNA immunoprecipitation

Isolation of TTP-associated mRNAs under native conditions was performed essentially as described previously (Gama-Carvalho *et al*, 2006) with modifications. Briefly, the precleared extract of 1 × 10⁷ TTP^{-/-} or WT primary macrophages was immunoprecipitated using TTP antiserum or preimmune serum control for 1 h at 4°C. Immune complexes were precipitated using protein A sepharose beads (GE Healthcare) coated with tRNA and RNase-free bovine serum albumin (Ambion) by rotating for 1 h at 4°C. After three washing steps with lysis buffer, bound complexes were eluted using TES buffer (10 mmol/l Tris pH 8.0, 0.5 mmol/l EDTA, 0.5% SDS) at 65°C for 15 min. RNA was isolated and reverse transcribed as mentioned before. Samples were analyzed by RT–PCR performing 35 cycles using the primers shown in the primer list or as described for qRT–PCR.

Reagents

Rabbit antibody to TTP was used as described (Schaljo *et al*, 2009). pp38 MAPK and p38 MAPK antibodies were from Cell Signaling Technologies and Santa Cruz Biotechnology, respectively. LPS from *Escherichia coli* 055:B5 was used at a concentration of 10 ng/ml, act D and SB203580 (all from Sigma) were used at a concentration of 5 μg/ml and 4 μM, respectively.

Cell culture

HeLa Tet-Off cells (Clontech) were grown in DMEM supplemented with 10% FCS. BMDMs were grown in L cell-derived CSF-1 as described (Schaljo *et al*, 2009). For experiments with cells derived from TTP^{-/-} and WT mice, littermates from TTP^{+/-} colony were used. For experiments with cells derived from TTP^{ΔM} and TTP^{fl/fl} mice, littermates from TTP^{ΔM/fl} colony were used. Mice for bone marrow collection were 8–12 weeks old.

Western blot

After treatment, whole cell extracts were prepared and assayed by western blotting as described elsewhere (Schaljo *et al*, 2009).

Detection and quantitation of signals were performed using the infrared imaging system Odyssey (LI-Cor Biosciences).

Plasmids

pTetBBB/IL1 α , pTetBBB/Cxcl2 and pTetBBB/HPRT were created by insertion of the full-length 3' UTRs of *Il1a*, *Cxcl2* and *Hprt* into the *Bgl*II and *Bam*HI site located in the β -globin 3' UTR of the pTetBBB plasmid which was containing a TRE in the promoter (Ogilvie et al, 2005). The 3' UTRs were PCR cloned using the primers pIl1 fwd and pIl1 rev for *Il1a*, pCxcl2 fwd and pCxcl2 rev for *Cxcl2* and pHprt fwd and pHprt rev for *Hprt* (see primer list). For constitutive expression of TTP, murine TTP was expressed from the CMV promoter in the plasmid pCMV-TTP.

Primer list

p1: 5'-ATC TAG CTG ATC CAT ACT GGG-3';
p2: 5'-AGG TTC TCC CTG GAG TTT GTG TGA-3';
Murine *Hprt* fwd 5'-GGATTTGAATCACGTTTGTGTCAT-3';
Murine *Hprt* rev 5'-ACACCTGCTAATTTACTGGCAA-3';
Human *Hprt* fwd 5'-TGTGTGCTCAAGGGGGG-3';
Human *Hprt* rev 5'-CGTGGGTCCTTTTCACC-3';
Rabbit β -globin fwd 5'-TCCTAAGGTGAAGGCTCATGGCAA-3';
Rabbit β -globin rev 5'-GTGGTATTGTGAGCCAGGGCATT-3';
Murine *TNF* fwd 5'-TTCTGTCTACTGAACTTCGGGGTGATCGGTCC-3';
Murine *TNF* rev 5'-GTATGAGATAGCAAATCGGCTGACGGTGTGGG-3';
Murine *IL6* fwd 5'-ATGGATGCTACCAAAGTGGAT-3';
Murine *IL6* rev 5'-TGAAGGACTCTGGCTTTGTCT-3';
pIl1a fwd 5'-TTTTTTGGATCCGAGCCTTATTTCCGGGAGTCTA-3';
pIl1a rev 5'-TTTTTTAGATCTGTGATAGTTACATGACACTGTGG-3';
pCxcl2 fwd 5'-TTTTTTGGATCCGAAAGGAGGAGCCTGGGCTG-3';
pCxcl2 rev 5'-TTTTTTAGATCTCATGAATAAATAAATGTGTCCACTTC-3';
pHprt fwd 5'-TTTTTTGGATCCTGAGCGCAAGTTGAATCTGCA-3';
pHprt rev 5'-TTTTTTAGATCTATTTAAAGGAAGTGTGACAACG-3';
Ccl2 fwd 5'-AGCCAGATGCAAGTAAACGCC-3';
Ccl2 rev 5'-ATCTCATTGGTTCCGATCCAGG-3';
Ccl4 fwd 5'-TGTTCTCTTACACCTCCCGG-3';
Ccl4 rev 5'-AAGAAGAGGGCAGGAAATCTG-3';
Ccl7 fwd 5'-GCATCCACATGCTGCTATGTC-3';
Ccl7 rev 5'-CAGTTCTCAGAAAGAACAGCG-3';
Ets2 fwd 5'-AAA GGA GCA ACG ACG TCT TG-3';
Ets2 rev 5'-CGT TGA GGT GAG AGT TTT CCT C-3';
Junb: QuantiTect Primer Assay (Qiagen) QT00241892
Plaur fwd 5'-TGA AGT GGT GAC CCT CCA GAG-3';
Plaur rev 5'-TTG ATG AGA GAC GCC TCT TCG-3';
Il6 fwd 5'-ATG GAT GCT ACC AAA CTG GAT-3';
Il6 rev 5'-TGA AGG ACT CTG GCT TTG TCT-3';
Tnfs9 fwd 5'-CCA ACA CTA CAC AAC AGG GCT-3';
Tnfs9 rev 5'-TAG TAG AGC CCG GGA CTG TC-3';
TTP fwd 5'-CTCTGCCATCTACGAGAGCC-3';
TTP rev 5'-GATGGAGTCCGAGTTTATGTTCC-3'.

Statistical analysis

For microarray data, a linear model analysis with genotype (WT versus TTP^{-/-}), treatment (0, 45 and 90 min), their interaction and individual as independent variables was fitted. Residuals were plotted, visually inspected and tested for normality. Design matrices were specified such that the coefficients for the relevant comparisons could be calculated, e.g., between the baseline and induced states and between genotypes. Only the significance levels are reported. For qRT-PCR data, normalized copy numbers were log-transformed, and mean values and standard errors of the mean (s.e.m.) were calculated (for *n* as described in the figure legends). Statistical significance of differences in mRNA and cytokine levels in LPS-treated animals were calculated using *T* test (**P*<0.05; ***P*<0.01; ****P*<0.001). Kaplan-Meier survival analysis was employed in LPS-induced endotoxin shock model.

Supplementary information

Supplementary information is available at the *Molecular Systems Biology* website (www.nature.com/msb).

Acknowledgements

We wish to thank Perry Blackshear for providing TTP^{-/-} mice; Thomas Kolbe for excellent assistance with animal breeding; Paul Bohjanen for providing beta-globin reporter vector; Peter J Murray, Birgit Strobl, Christoph Schüller and Amanda Jamieson for critical reading of the manuscript. The study was funded by the Austrian Science Fund (FWF) grants SFB F28 to PK and MM and W1220-B09 DP 'Molecular Mechanisms of Cell Signaling' to PK, the University of Vienna Research platform 323500 to PK and IH, the Austrian Federal Ministry of Science and Research Program GEN-AU II/III project 'Austrian Network for Functional Genomics of the Mouse' to TR and MM, and Deutsche Forschungsgemeinschaft SFB 643, TP A10 to RL.

Author contributions: FK designed experiments, did most of the experimental studies and drafted the manuscript; CM cloned reporter plasmids and did reporter assays; CV did computational analysis and statistics of microarrays; FE and VS validated several TTP target mRNAs; RVMK, TR and MM generated and provided reagents; ARG and IH did 3' UTR analysis; HH did RNA-EMSA studies; RL did microarray experiments and computational analysis; and PK designed experiments, supervised the study and wrote the manuscript.

Conflict of interest

The authors declare that they have no conflict of interest.

References

- Abdelmohsen K, Lal A, Kim HH, Gorospe M (2007) Posttranscriptional orchestration of an anti-apoptotic program by HuR. *Cell Cycle* **6**: 1288–1292
- Anderson P (2010) Post-transcriptional regulons coordinate the initiation and resolution of inflammation. *Nat Rev* **10**: 24–35
- Barreau C, Paillard L, Osborne HB (2005) AU-rich elements and associated factors: are there unifying principles? *Nucleic Acids Res* **33**: 7138–7150
- Berg DJ, Kuhn R, Rajewsky K, Muller W, Menon S, Davidson N, Grunig G, Rennick D (1995) Interleukin-10 is a central regulator of the response to LPS in murine models of endotoxin shock and the Shwartzman reaction but not endotoxin tolerance. *J Clin Invest* **96**: 2339–2347
- Blackshear PJ (2002) Tristetraprolin and other CCCH tandem zinc-finger proteins in the regulation of mRNA turnover. *Biochem Soc Trans* **30** (Part 6): 945–952
- Blackshear PJ, Lai WS, Kennington EA, Brewer G, Wilson GM, Guan X, Zhou P (2003) Characteristics of the interaction of a synthetic human tristetraprolin tandem zinc finger peptide with AU-rich element-containing RNA substrates. *J Biol Chem* **278**: 19947–19955
- Cairrao F, Halees AS, Khabar KS, Morello D, Vanzo N (2009) AU-rich elements regulate Drosophila gene expression. *Mol Cell Biol* **29**: 2636–2643
- Carballo E, Lai WS, Blackshear PJ (1998) Feedback inhibition of macrophage tumor necrosis factor- α production by tristetraprolin. *Science* **281**: 1001–1005
- Carballo E, Lai WS, Blackshear PJ (2000) Evidence that tristetraprolin is a physiological regulator of granulocyte-macrophage colony-stimulating factor messenger RNA deadenylation and stability. *Blood* **95**: 1891–1899
- Cheadle C, Fan J, Cho-Chung YS, Werner T, Ray J, Do L, Gorospe M, Becker KG (2005) Stability regulation of mRNA and the control of gene expression. *Ann NY Acad Sci* **1058**: 196–204
- Chekulaeva M, Filipowicz W (2009) Mechanisms of miRNA-mediated post-transcriptional regulation in animal cells. *Curr Opin Cell Biol* **21**: 452–460
- Chen YL, Huang YL, Lin NY, Chen HC, Chiu WC, Chang CJ (2006) Differential regulation of ARE-mediated TNF α and IL-1 β mRNA stability by lipopolysaccharide in RAW264.7 cells. *Biochem Biophys Res Commun* **346**: 160–168

- Clausen BE, Burkhardt C, Reith W, Renkawitz R, Forster I (1999) Conditional gene targeting in macrophages and granulocytes using LysMcre mice. *Transgenic Res* **8**: 265–277
- Dahan O, Gingold H, Pilpel Y (2011) Regulatory mechanisms and networks couple the different phases of gene expression. *Trends Genet* **27**: 316–322
- Datta S, Biswas R, Novotny M, Pavicic Jr PG., Herjan T, Mandal P, Hamilton TA (2008) Tristetraprolin regulates CXCL1 (KC) mRNA stability. *J Immunol* **180**: 2545–2552
- Emmons J, Townley-Tilson WH, Deleault KM, Skinner SJ, Gross RH, Whitfield ML, Brooks SA (2008) Identification of TTP mRNA targets in human dendritic cells reveals TTP as a critical regulator of dendritic cell maturation. *RNA* **14**: 888–902
- Frasca D, Landin AM, Alvarez JP, Blackshear PJ, Riley RL, Blomberg BB (2007) Tristetraprolin, a negative regulator of mRNA stability, is increased in old B cells and is involved in the degradation of E47 mRNA. *J Immunol* **179**: 918–927
- Gama-Carvalho M, Barbosa-Morais NL, Brodsky AS, Silver PA, Carmo-Fonseca M (2006) Genome-wide identification of functionally distinct subsets of cellular mRNAs associated with two nucleocytoplasmic-shuttling mammalian splicing factors. *Genome Biol* **7**: R113
- Ghosh M, Aguila HL, Michaud J, Ai Y, Wu MT, Hemmes A, Ristimaki A, Guo C, Furneaux H, Hla T (2009) Essential role of the RNA-binding protein HuR in progenitor cell survival in mice. *J Clin Invest* **119**: 3530–3543
- Grivnennikov SI, Tumanov AV, Liepinsh DJ, Kruglov AA, Marakusha BI, Shakhov AN, Murakami T, Drutska LN, Forster I, Clausen BE, Tassarollo L, Ryffel B, Kuprash DV, Nedospasov SA (2005) Distinct and nonredundant *in vivo* functions of TNF produced by t cells and macrophages/neutrophils: protective and deleterious effects. *Immunity* **22**: 93–104
- Gruber AR, Fallmann J, Kratochvill F, Kovarik P, Hofacker IL (2011) AREsite: a database for the comprehensive investigation of AU-rich elements. *Nucleic Acids Res* **39** (Database issue): D66–D69
- Hammer M, Mages J, Dietrich H, Schmitz F, Striebel F, Murray PJ, Wagner H, Lang R (2005) Control of dual-specificity phosphatase-1 expression in activated macrophages by IL-10. *Eur J Immunol* **35**: 2991–3001
- Hammer M, Mages J, Dietrich H, Servatius A, Howells N, Cato AC, Lang R (2006) Dual specificity phosphatase 1 (DUSP1) regulates a subset of LPS-induced genes and protects mice from lethal endotoxin shock. *J Exp Med* **203**: 15–20
- Hao S, Baltimore D (2009) The stability of mRNA influences the temporal order of the induction of genes encoding inflammatory molecules. *Nat Immunol* **10**: 281–288
- Hodson DJ, Janas ML, Galloway A, Bell SE, Andrews S, Li CM, Pannell R, Siebel CW, MacDonald HR, De Keersmaecker K, Ferrando AA, Grutz G, Turner M (2010) Deletion of the RNA-binding proteins ZFP36L1 and ZFP36L2 leads to perturbed thymic development and T lymphoblastic leukemia. *Nat Immunol* **11**: 717–724
- Horner TJ, Lai WS, Stumpo DJ, Blackshear PJ (2009) Stimulation of polo-like kinase 3 mRNA decay by tristetraprolin. *Mol Cell Biol* **29**: 1999–2010
- Hume DA, Wells CA, Ravasi T (2007) Transcriptional regulatory networks in macrophages. *Novartis Found Symp* **281**: 2–18; discussion 18–24, 50–13, 208–209
- Jalonen U, Nieminen R, Vuolteenaho K, Kankaanranta H, Moilanen E (2006) Down-regulation of tristetraprolin expression results in enhanced IL-12 and MIP-2 production and reduced MIP-3 α synthesis in activated macrophages. *Mediators Inflamm* **2006**: 40691
- Kontoyiannis D, Pasparakis M, Pizarro TT, Cominelli F, Kollias G (1999) Impaired on/off regulation of TNF biosynthesis in mice lacking TNF AU-rich elements: implications for joint and gut-associated immunopathologies. *Immunity* **10**: 387–398
- Lai WS, Carballo E, Thorn JM, Kennington EA, Blackshear PJ (2000) Interactions of CCCH zinc finger proteins with mRNA. Binding of tristetraprolin-related zinc finger proteins to Au-rich elements and destabilization of mRNA. *J Biol Chem* **275**: 17827–17837
- Lai WS, Parker JS, Grissom SF, Stumpo DJ, Blackshear PJ (2006) Novel mRNA targets for tristetraprolin (TTP) identified by global analysis of stabilized transcripts in TTP-deficient fibroblasts. *Mol Cell Biol* **26**: 9196–9208
- Litvak V, Ramsey SA, Rust AG, Zak DE, Kennedy KA, Lampano AE, Nykter M, Shmulevich I, Aderem A (2009) Function of C/EBP δ in a regulatory circuit that discriminates between transient and persistent TLR4-induced signals. *Nat Immunol* **10**: 437–443
- Mages J, Dietrich H, Lang R (2007) A genome-wide analysis of LPS tolerance in macrophages. *Immunobiology* **212**: 723–737
- Morrison TB, Weis JJ, Wittwer CT (1998) Quantification of low-copy transcripts by continuous SYBR Green I monitoring during amplification. *Biotechniques* **24**: 954–958, 960, 962
- Mukherjee N, Lager PJ, Friedersdorf MB, Thompson MA, Keene JD (2009) Coordinated posttranscriptional mRNA population dynamics during T-cell activation. *Mol Syst Biol* **5**: 288
- Murray PJ (2005) The primary mechanism of the IL-10-regulated antiinflammatory response is to selectively inhibit transcription. *Proc Natl Acad Sci USA* **102**: 8686–8691
- Ogilvie RL, Abelson M, Hau HH, Vlasova I, Blackshear PJ, Bohjanen PR (2005) Tristetraprolin down-regulates IL-2 gene expression through AU-Rich element-mediated mRNA decay. *J Immunol* **174**: 953–961
- Ogilvie RL, Sternjohn JR, Rattenbacher B, Vlasova IA, Williams DA, Hau HH, Blackshear PJ, Bohjanen PR (2009) Tristetraprolin mediates interferon-gamma mRNA decay. *J Biol Chem* **284**: 11216–11223
- Puig S, Askeland E, Thiele DJ (2005) Coordinated remodeling of cellular metabolism during iron deficiency through targeted mRNA degradation. *Cell* **120**: 99–110
- Raghavan A, Bohjanen PR (2004) Microarray-based analyses of mRNA decay in the regulation of mammalian gene expression. *Brief Funct Genomic Proteomic* **3**: 112–124
- Sandler H, Stoecklin G (2008) Control of mRNA decay by phosphorylation of tristetraprolin. *Biochem Soc Trans* **36**(Part 3): 491–496
- Schaljo B, Kratochvill F, Gratz N, Sadzak I, Sauer I, Hammer M, Vogl C, Strobl B, Muller M, Blackshear PJ, Poli V, Lang R, Murray PJ, Kovarik P (2009) Tristetraprolin is required for full anti-inflammatory response of murine macrophages to IL-10. *J Immunol* **183**: 1197–1206
- Smyth GK (2004) Linear models and empirical Bayes methods for assessing differential expression in microarray experiments. *Stat Appl Genet Mol Biol* **3**: Article3
- Stoecklin G, Anderson P (2007) In a tight spot: ARE-mRNAs at processing bodies. *Genes Dev* **21**: 627–631
- Stoecklin G, Gross B, Ming XF, Moroni C (2003) A novel mechanism of tumor suppression by destabilizing AU-rich growth factor mRNA. *Oncogene* **22**: 3554–3561
- Stoecklin G, Stoeckle P, Lu M, Muehleemann O, Moroni C (2001) Cellular mutants define a common mRNA degradation pathway targeting cytokine AU-rich elements. *RNA* **7**: 1578–1588
- Stoecklin G, Tenenbaum SA, Mayo T, Chittur SV, George AD, Baroni TE, Blackshear PJ, Anderson P (2008) Genome-wide analysis identifies interleukin-10 mRNA as target of tristetraprolin. *J Biol Chem* **283**: 11689–11699
- Taylor GA, Carballo E, Lee DM, Lai WS, Thompson MJ, Patel DD, Schenkman DI, Gilkeson GS, Broxmeyer HE, Haynes BF, Blackshear PJ (1996) A pathogenetic role for TNF α in the syndrome of cachexia, arthritis, and autoimmunity resulting from tristetraprolin (TTP) deficiency. *Immunity* **4**: 445–454
- Tchen CR, Brook M, Saklatvala J, Clark AR (2004) The stability of tristetraprolin mRNA is regulated by mitogen activated protein kinase p38 and by tristetraprolin itself. *J Biol Chem* **279**: 32393–32400
- Tudor C, Marchese FP, Hitti E, Aubareda A, Rawlinson L, Gaestel M, Blackshear PJ, Clark AR, Saklatvala J, Dean JL (2009) The p38 MAPK pathway inhibits tristetraprolin-directed decay

of interleukin-10 and pro-inflammatory mediator mRNAs in murine macrophages. *FEBS Lett* **583**: 1933–1938

von Roretz C, Gallouzi IE (2008) Decoding ARE-mediated decay: is microRNA part of the equation? *J Cell Biol* **181**: 189–194

Wakeland E, Morel L, Achey K, Yui M, Longmate J (1997) Speed congenics: a classic technique in the fast lane (relatively speaking). *Immunol Today* **18**: 472–477

Worthington MT, Pelo JW, Sachedina MA, Applegate JL, Arseneau KO, Pizarro TT (2002) RNA binding properties of the AU-rich element-binding recombinant Nup475/TIS11/tristetraprolin protein. *J Biol Chem* **277**: 48558–48564

Zhao W, Liu M, D'Silva NJ, Kirkwood KL (2011) Tristetraprolin regulates interleukin-6 expression through p38 MAPK-dependent affinity changes with mRNA 3' untranslated region. *J Interferon Cytokine Res* **31**: 629–637



Molecular Systems Biology is an open-access journal published by *European Molecular Biology Organization* and *Nature Publishing Group*. This work is licensed under a Creative Commons Attribution-Noncommercial-Share Alike 3.0 Unported License.